Design, synthesis and biological evaluation of 2-alkoxycarbonyl-3-anilinoindoles as a new class of potent inhibitors of tubulin polymerization

Romeo Romagnoli[a,*], Filippo Prencipe[a], Paola Oliva[a], Maria Kimatrai Salvador[a], Andrea Brancale[b], Salvatore Ferla[b], Ernest Hamel[c], Giampietro Viola[d,e], Roberta Bortolozzi[d], Leentje Persoons[f], Jan Balzarini[f], Sandra Liekens[f], Dominique Schols[f]

[a] *Dipartimento di Scienze Chimiche e Farmaceutiche, Università di Ferrara, 44121 Ferrara, Italy*
[b] *School of Pharmacy and Pharmaceutical Sciences, Cardiff University, King Edward VII Avenue, Cardiff, CF10 3NB, UK*
[c] *Screening Technologies Branch, Developmental Therapeutics Program, Division of Cancer Treatment and Diagnosis, Frederick National Laboratory for Cancer Research, National Cancer Institute, National Institutes of Health, Frederick, MD 21702, USA*
[d] *Dipartimento di Salute della Donna e del Bambino, Laboratorio di Oncoematologia, Università di Padova, 35131 Padova, Italy*
[e] *Istituto di Ricerca Pediatrica (IRP), Corso Stati Uniti 4, 35128 Padova, Italy*
[f] *Rega Institute for Medical Research, KU Leuven, Laboratory of Virology and Chemotherapy, Leuven, Belgium*

ARTICLE INFO

Keywords:
Microtubules
Structure-activity relationship
Indole
Antiproliferative activity
Tubulin

ABSTRACT

A new class of inhibitors of tubulin polymerization based on the 2-alkoxycarbonyl-3-(3′,4′,5′-trimethoxyanilino) indole molecular skeleton was synthesized and evaluated for antiproliferative activity, inhibition of tubulin polymerization and cell cycle effects. The results presented show that the methoxy substitution and location on the indole nucleus plays an important role in inhibition of cell growth, and the most favorable position for the substituent was at C-6. In addition, a small-size ester function (methoxy/ethoxycarbonyl) at the 2-position of the indole core was desirable. Also, analogues that were alkylated with methyl, ethyl or *n*-propyl groups or had a benzyl moiety on the *N*-1 indolic nitrogen retained activity equivalent to those observed in the parent *N*-1*H* analogues. The most promising compounds of the series were 2-methoxycarbonyl-3-(3′,4′.5′-trimethoxyanilino)-5-methoxyindole **3f** and 1-methyl-2-methoxycarbonyl-3-(3′,4′.5′-trimethoxyanilino)-6-methoxy-indole **3w**, both of which target tubulin at the colchicine site with antitubulin activities comparable to that of the reference compound combretastatin A-4.

1. Introduction

Microtubules are polymeric structures composed of two structurally similar protein subunits, α- and β-tubulin, which form heterodimers arranged head-to-tail in a linear protofilament, with 13 protofilaments forming the cylindrical microtubule. They are crucial in a number of cellular functions critical to the life cycle of the cell [1,2].

The biological importance of microtubules makes them an interesting target for the development of clinically useful anticancer drugs [3,4], as has been demonstrated by the therapeutic use of vinca alkaloids and taxanes [5–7]. Compounds such as vinca alkaloids that are able to interfere with the assembly of tubulin into microtubules have antimitotic activity and are referred to as tubulin polymerization inhibitors [8]. In contrast, taxanes prevent microtubule disassembly and are classified as microtubule stabilizing agents [9].

Numerous chemically diverse antimitotic agents, many of which are natural products, interact specifically with tubulin and alter tubulin polymerization [10–12]. Combretastatin A-4 (CA-4, **1a**, Fig. 1), isolated from the bark of the South African tree *Combretum caffrum*, is one of the well-known natural tubulin binding molecules affecting microtubule dynamics [13]. CA-4 potently inhibited the polymerization process of tubulin into microtubules by binding to the colchicine site on tubulin, hampering the formation of the mitotic spindle [14]. CA-4 also displayed potent cytotoxic activities against a wide variety of human cancer cell lines at low nanomolar concentrations, including those that are multidrug-resistant [15]. The water-soluble disodium phosphate prodrug of CA-4 (CA-4P, **1b**) showed promising results as a tumor vascular-disrupting agent (VDA) in phase II clinical trials for multi-drug combination antitumor therapy [16–18]. Its structural simplicity, along with its ability to selectively damage tumor neovasculature, makes CA-4 of great interest from the medicinal chemistry point of view, and a wide number of CA-4 analogues have been developed and evaluated in

* Corresponding author.
E-mail address: rmr@unife.it (R. Romagnoli).

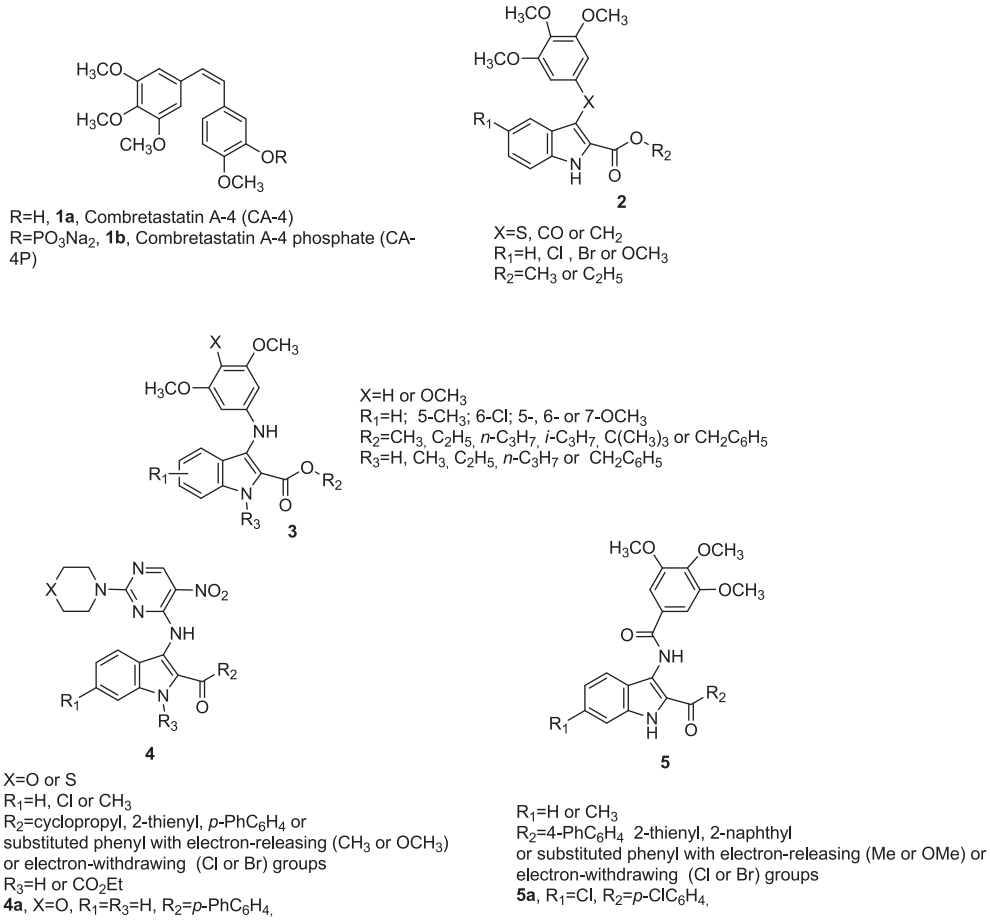

Fig. 1. Structures of CA-4 (**1a**) and CA-4P (**1b**). General structures **2**, **4** and **5** of various known indoles and of 2-alkoxycarbonyl-3-anilinoindoles (**3**) described in this manuscript.

structure–activity relationship (SAR) studies [19–22].

Several synthetic molecules have also been reported as tubulin destabilizing agents, acting as inhibitors of tubulin polymerization [23–27]. In this respect, a literature search revealed past [28–31] and recent [32–34] studies in which the indole molecular skeleton has been widely employed as a versatile pharmacophore for the development of chemically diverse small molecules identified as tubulin polymerization inhibitors.

Among the synthetic inhibitors of tubulin polymerization having an indole as their core nucleus, it was observed that the presence of an alkoxycarbonyl function at the 2-position of the *N*-1-*H*-indole system was essential for potent antitumor activity and for potent inhibition of tubulin polymerization. A series of 2-alkoxycarbonyl-3-(3′,4′,5′-trimethoxy-phenylthio/benzoyl/benzyl)-1*H*-indole derivatives with general structure **2** was reported as antitubulin agents by Silvestri and coworkers [35–37]. These compounds were characterized by the presence of an electron-withdrawing atom (Cl or Br) or the electron-donating methoxy group at the C-5 position and a methoxy/ethoxycarbonyl moiety at the C-2 position of the indole ring, with the greatest inhibitory effects on MCF-7 cells observed for either sulfur or carbonyl derivatives bearing a 2-methoxycarbonyl group at the 2-position of the indole.

Therefore, in continuation on our work on anticancer agents based on the indole skeleton, in an effort to further improve activity and extend the SAR evaluation of derivatives with general structure **2**, we focused our attention on exploring the possibility of replacing the sulfur, carbonyl or methylene bridging units between the 3-position of the indole nucleus and the 3′,4′,5′-trimethoxyphenyl or 3′,5′-dimethoxyphenyl moieties by a bioisosteric anilinic nitrogen (NH) moiety with hydrogen-bond accepting and donating capability to furnish a new series of 2-alkoxycarbonyl-3-(3′,4′,5′-trimethoxy/2′,5′-dimethoxyanilino)indole derivatives with general structure **3** modified with respect to positions C-5 to C-7 with methyl, chloro or methoxy moieties.

Once the 3′,4′,5′-trimethoxyanilino or 3′,5′-dimethoxyanilino moiety was placed at the 3-position of the indole core, we explored the SAR by examining the following modifications:

(a) various substitutions at the *N*-1 position (we selected hydrogen, methyl, ethyl, propyl or benzyl to examine the steric effect of substituent R_3);
(b) the effect of the electron-withdrawing 2-alkoxycarbonyl group esters with either a linear or a branched alkoxy chain (R_2 = methyl, ethyl, *n*-propyl, *i*-propyl, *t*-butyl or benzyl);
(c) the location of the methoxy group (R_1) at the 5-, 6- or 7-position of the indole nucleus as well as the presence of an electron-releasing methyl or electron-withdrawing chlorine atom at the C-5 or C-6 position, respectively.

Recently, a series of 2-aroyl-3-aminopyrimidine-1*H*-indole derivatives with general structure **4**, possessing a morpholine or thiomorpholine linked to the C-2 position of the pyrimidine ring were synthesized by Zhao et al. [38]. Among the tested compounds, the most promising was derivative **4a**, with IC_{50} values of 0.29, 4.04, and 9.48 μM against the MCF-7, HeLa, and HCT116 cell lines, respectively. The same derivative also exhibited the most potent anti-tubulin activity, with an IC_{50} of 19.3 μM in their tubulin polymerization assay.

The same authors also reported a series of 2-aroyl-3-(3′,4′,5′-trimethoxybenzoyl)amino-1*H*-indoles with general structure **5**

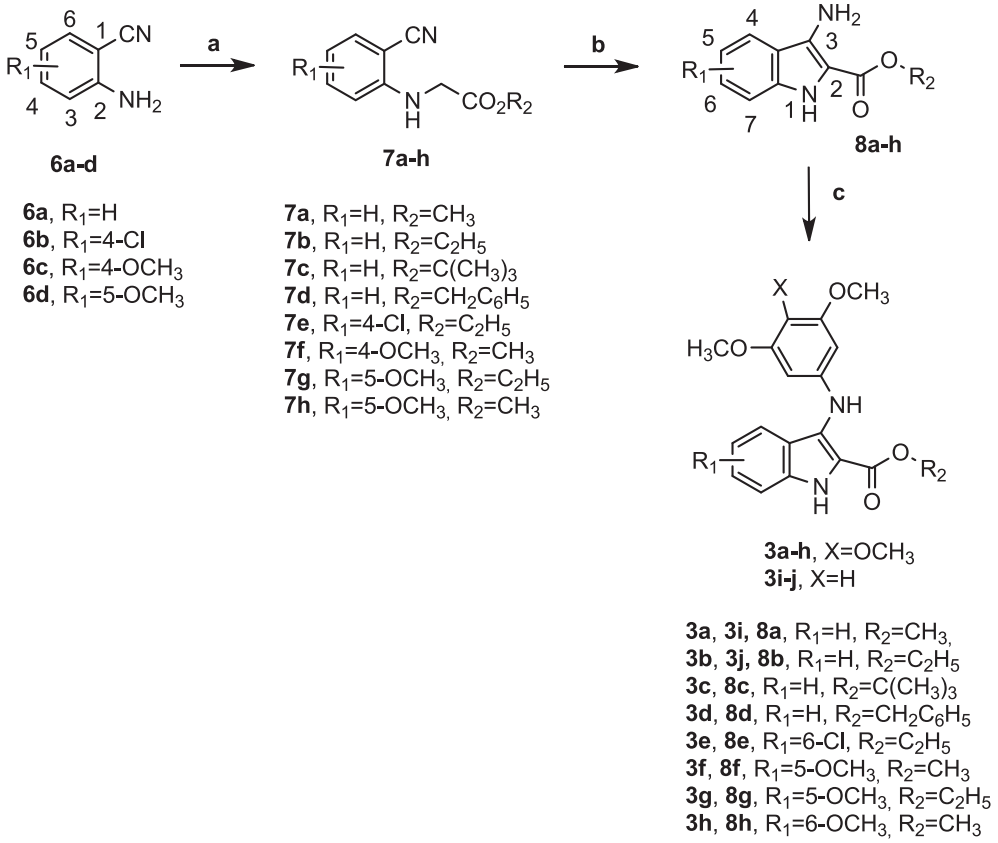

Scheme 1. Reagents. **a**: bromoacetate esters, $NaHCO_3$, appropriate solvent, reflux, 24 h; **b**: *t*-BuOK, THF, rt, 2 h; **c**: 1-bromo-3,4,5-trimethoxybenzene or 1-bromo-3,5-dimethoxybenzene for the synthesis of **3a-h** and **3i-j**, respectively, $Pd(OAc)_2$, BINAP, Cs_2CO_3, PhMe, 100 °C, 16 h.

incorporating an amido bridge into the 3-position of the indole nucleus [39]. The most active derivative **5a** inhibited the growth of the T47D, BT549, and MDA-MB-231 cell lines with IC_{50} values of 0.04, 3.17, and 6.43 μM, respectively, and showed moderate antitubulin polymerization activity with an IC_{50} of 9.5 μM.

2. Chemistry

3-Amino-2-alkoxycarbonyl-1*H*-indoles **8a-h** were synthesized in acceptable yields by Thorpe-Zigler cyclization of the corresponding *N*-aryl glycinate esters **7a-h** using *t*-BuOK as base in THF. These latter intermediates were prepared starting from anthranilonitriles **6a-d** by the reaction with the appropriate bromoacetate esters under basic medium ($NaHCO_3$). Finally, the novel derivatives **3a-j** were prepared using the C—N Buchwald-Hartwig palladium catalyzed cross-coupling protocol, by reaction of 3-amino-1*H*-indole analogues **8a-h** with 1-bromo-3,4,5-trimethoxybenzene or 1-bromo-3,5-dimethoxybenzene, in the presence of $Pd(OAc)_2$, *rac*-BINAP and Cs_2CO_3 (as catalyst, ligand and base, respectively) in toluene at 100 °C (Scheme 1).

N-1-alkyl/benzyl indole derivatives **3k-ac** were prepared by the synthetic route outlined in Scheme 2. The 2-alkoxycarbony-1*H*-indole derivatives **9a-g** were regioselectively brominated at the 3-position with *N*-bromosuccinimide (NBS) in DMF as solvent to furnish the corresponding 3-bromo-1*H*-indole analogues **10a-g** in almost quantitative yield. The *N*-1 substituted compounds **11a-p** were synthesized in good yields by the condensation of N-1*H*-indole analogues **10a-g** with the appropriate alkyl (methyl, ethyl or *n*-propyl) iodide or benzyl bromide using NaH as base in DMF. The subsequent Buchwald-Hartwig reaction of the key building blocks *N*-alkyl and *N*-benzyl indole derivatives **11a-p** with 3,4,5-trimethoxyaniline or 3,5-dimethoxyaniline, following the identical protocol reported for the preparation of compounds **3a-j**, provided final derivatives **3k-ac** in acceptable yields.

3. Biological results and discussion

3.1. In vitro antiproliferative activities

The synthesized 2-alkoxycarbonyl-3anilinoindoles **3a-c** were evaluated for their ability to inhibit the growth of a panel of four human cancer cell lines, cervix carcinoma (HeLa), colon adenocarcinoma (HT29), breast adenocarcinoma (MCF-7) and promyelocytic leukemia (HL-60) cells. The results are summarized in Table 1, using CA-4 (**1a**) as the positive control. In general, the human promyelocytic leukemia HL-60 cell line was less sensitive to these compounds as compared with the HeLa, HT29 and MCF-7 cells. In contrast, the HL-60 cells were more sensitive than the other three lines towards the control compound CA-4.

The data in Table 1 showed that, among the twenty-nine synthesized compounds, the most active derivatives (with the exception of 2-ethoxycarbonyl derivative **3q**) were found among the 2-methoxyxycarbonyl indoles **3h**, **3p**, **3x** and **3y**, with antiproliferative activity lower than 1 μM against all cancer cell lines. Compound **3y**, with the *N*-1-benzyl-2-methoxycarbonyl-6-methoxy-indole moiety was the most potent compound of the series, with antiproliferative IC_{50} values ranging from 0.055 to 0.17 μM against the panel of cancer cell lines. Compounds **3h**, **3p** and **3x** had nearly equivalent activity, with IC_{50} values of 0.065–0.49, 0.36–0.77 and 0.063–0.93 μM, respectively). In addition, derivatives **3a**, **3f-g**, **3k**, **3q**, **3s**, **3w** and **3aa** also showed excellent antiproliferative activity against the HeLa, HT29 and MCF-7 cancer cell lines, with submicromolar IC_{50} values. Half of the synthesized compounds, with IC_{50} values lower than 1 μM against the HT29 cell line, were 3–18-fold more potent than CA-4 against this cell line, with **3aa** and **3y** as the most active derivatives of the series (IC_{50}:0.17 μM), while almost one-third of prepared molecules (**3g-h**, **3m**, **3w-y** and **3aa**) were 2–7-fold more active than CA-4 against MCF-7 cells (IC_{50}s of 0.055–0.23 μM versus 0.37 μM for CA-4). Moreover, all

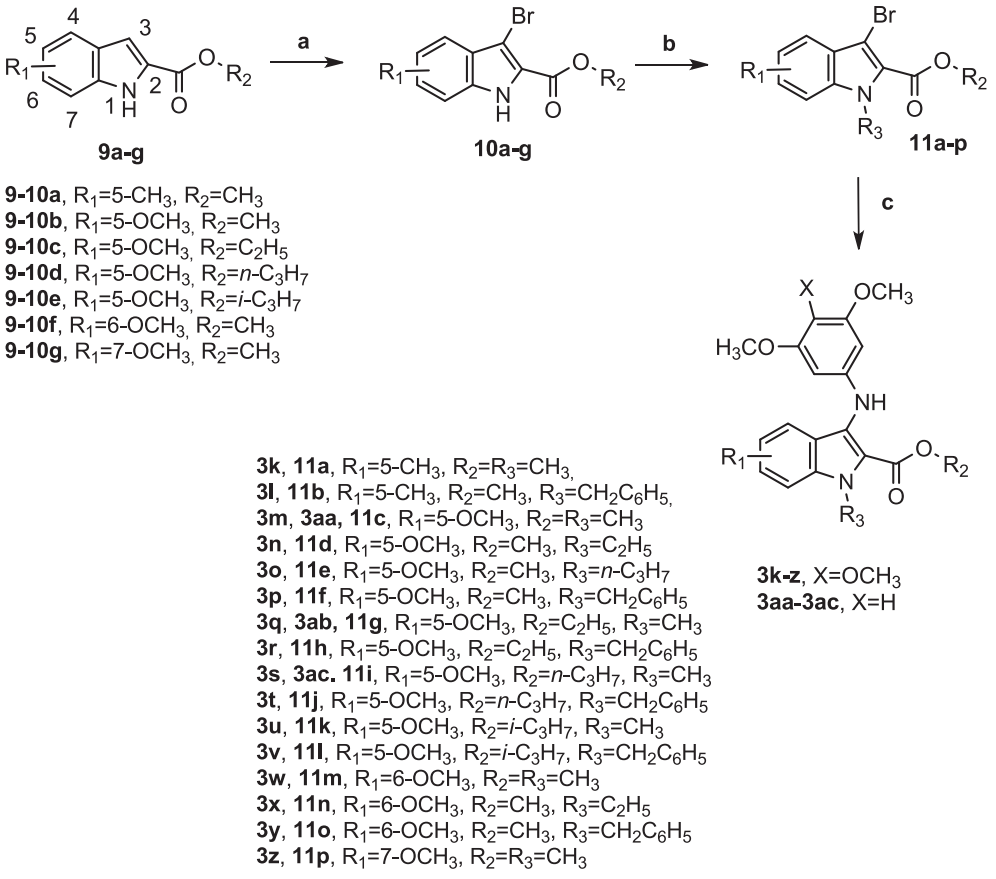

Scheme 2. Reagents. Reagents. **a**: NBS, DMF, rt, 2 h; **b**: appropriate alkyl iodide or benzyl bromide, NaH, DMF, rt, 2 h; **c**: 3,4,5-trimethoxyaniline or 3,5-dimethoxyaniline for the synthesis of **3k-z** and **3aa-ac**, respectively, $Pd(OAc)_2$, BINAP, Cs_2CO_3, PhMe, 100 °C, 16 h.

synthesized molecules showed substantially reduced activity relative to **CA-4** against HeLa and HL-60 cancer cells (IC_{50}: 4 and 1 nM, respectively).

For the derivative **3a**, the IC_{50} values ranged from 0.47 to 0.8 μM against three of the four cancer cell lines. The elongation of the alkyl chain of 2-alkoxycarbonyl function of compound **3a** from methyl to ethyl, to yield **3b**, has a contrasting effect, with 1.5- and 2-fold reductions of activity on HT-29 and MCF-7 cells, respectively, and a 2- and 2.5-fold increased activity against HeLa and HL-60 cells, respectively. For compounds **3a** and **3b**, replacing a 3,4,5-trimethoxy phenyl ring with a 3,5-dimethoxyphenyl moiety (compounds **3i** and **3j**, respectively) caused a reduction of activity (1.5–12-fold) in all cell lines.

Replacement of methyl or ethyl of the 2-alkoxycarbonyl moiety on the 1*H*-indole nucleus of compounds **3a** and **3b** with a more bulky *t*-butyl or benzyl substituent (compounds **3c** and **3d**, respectively) resulted in a dramatic loss of potency (IC_{50} > 10 μM), thus revealing a steric effect of the substituent at the C-2 position of the indole ring on cell growth inhibitory activity.

The introduction of the electron-withdrawing chlorine atom at the C-6 position of the 1*H*-indole nucleus of compound **3b**, to yield derivative **3e**, caused a 3- and 5-fold reduction of activity against HT-29 and HeLa cells, respectively, while a 1.5- and 3-fold increase of activity was observed against HL-60 and MCF-7 cells.

The methoxy substituent on the benzene portion of the indole moiety, as well as the absence or presence of alkyl or benzyl substituents on the indole nitrogen, play an important role in affecting antiproliferative activity.

The introduction of a methoxy group at the C-5 position of derivative **3a**, to yield **3f**, increased from 1.5 to 3-fold the cell growth inhibitory activity relative to **3a** against HeLa, MCF-7 and HL-60 cells, with a 1.5-fold reduced activity against HT29 cells.

Homologation of the alkyl chain of the alkoxycarbonyl group by an extra methylene unit, from methyl to ethyl (compounds **3f** and **3g**, respectively), increased antiproliferative activity 2- and 5-fold against HT-29 and MCF-7 cells, respectively, while the 2-ethoxycarbonyl-1*H*-indole derivative **3g** was 5-fold less potent than **3f** against HL-60 cells, and the two derivatives proved equipotent against HeLa cells. For compound **3f**, moving the methoxy group from the 5-to the 6-position of the 1-*H*-indole ring (derivative **3h**) increased activity 2–8-fold against the whole panel of cancer cell lines.

Through the synthesis of compounds **3k-ac**, we investigated whether the introduction of a methyl, ethyl, *n*-propyl or benzyl moiety at the indole nitrogen of derivatives **3f-h** would lead to an increase or loss of activity through a steric effect. Starting from compound **3f**, the insertion of a methyl group at the *N*-1 position of the indole nucleus (**3m**) caused a 2.5-fold increase in antiproliferative activity relative to **3f** against MCF-7 cells, while the two derivatives were equipotent against the other cancer cell lines. Replacement of the C-5 methoxy of **3m** with a weak electron-releasing methyl group (**3k**), increased potency 2.5 and 3-fold against HT-29 and HeLa cells, respectively, while a strong reduction in activity (27-fold) was observed against HL-60 cells. For compound **3m**, replacement of the 3,4,5-trimethoxyphenyl ring with a 3,5-dimethoxy phenyl moiety (**3aa**) was well tolerated by the HeLa and MCF-7 cells, with the two compounds showing similar potency, while the latter compound was 9-fold more active than the former against HT-29 cells. In contrast, **3m** was 4-fold more potent than **3aa** against the HL-60 cell line.

Homologation of the *N*-1 alkyl chain on the indole nucleus from methyl to ethyl to *n*-propyl (compounds **3m**, **3n** and **3o**, respectively), maintained antiproliferative activity relative to the *N*-methyl derivative **3m** on the HeLa and HT-29 cell lines, while **3n** and **3o** were equipotent although half as potent as the *N*-1*H*-indole derivative **3m** against MCF-7

Table 1
In vitro inhibitory effects of compounds **3a-ac** and reference compound CA-4 (**1a**).

Compound	IC_{50} (μM)[a]			
	HeLa	HT29	MCF-7	HL-60
3a	0.8 ± 0.2	0.47 ± 0.04	0.74 ± 0.54	5.0 ± 1.1
3b	0.4 ± 0.03	0.74 ± 0.08	1.5 ± 0.6	1.9 ± 0.1
3c	> 10	> 10	> 10	> 10
3d	> 10	> 10	> 10	> 10
3e	2.1 ± 0.9	2.0 ± 0.3	0.44 ± 0.02	1.1 ± 0.0
3f	0.50 ± 0.22	0.96 ± 0.12	0.50 ± 0.38	1.4 ± 1.1
3g	0.60 ± 0.37	0.48 ± 0.34	0.10 ± 0.09	6.6 ± 3.3
3h	0.13 ± 0.04	0.47 ± 0.23	0.065 ± 0.054	0.49 ± 0.18
3i	1.4 ± 0.5	3.7 ± 2.8	0.40 ± 0.01	7.0 ± 1.0
3j	4.8 ± 4.5	8.7 ± 0.8	1.7 ± 0.2	7.8 ± 1.9
3k	0.19 ± 0.11	0.60 ± 0.26	0.37 ± 0.32	> 10
3l	1.8 ± 0.1	2.4 ± 1.2	0.74 ± 0.35	> 10
3m	0.62 ± 0.41	1.5 ± 0.5	0.20 ± 0.12	1.6 ± 1.0
3n	0.53 ± 0.44	1.1 ± 0.6	0.43 ± 0.20	1.7 ± 0.2
3o	0.60 ± 0.29	1.2 ± 0.5	0.45 ± 0.04	3.2 ± 1.0
3p	0.68 ± 0.30	0.77 ± 0.13	0.36 ± 0.16	0.60 ± 0.35
3q	0.60 ± 0.43	0.54 ± 0.30	0.38 ± 0.09	0.68 ± 0.12
3r	1.3 ± 0.6	1.7 ± 1.3	0.48 ± 0.25	0.64 ± 0.28
3s	0.95 ± 0.41	0.85 ± 0.15	0.62 ± 0.10	3.0 ± 0.11
3t	7.8 ± 1.7	5.3 ± 0.8	3.1 ± 2.1	2.6 ± 2.2
3u	> 10	> 10	> 10	> 10
3v	> 10	> 10	> 10	> 10
3w	0.54 ± 0.30	0.32 ± 0.03	0.11 ± 0.06	1.1 ± 0.7
3x	0.58 ± 0.32	0.93 ± 0.18	0.063 ± 0.017	0.10 ± 0.02
3y	0.13 ± 0.06	0.17 ± 0.02	0.055 ± 0.035	0.096 ± 0.054
3z	7.3 ± 2.2	1.7 ± 0.1	0.14 ± 0.08	8.1 ± 1.1
3aa	0.41 ± 0.19	0.17 ± 0.08	0.15 ± 0.04	6.2 ± 1.1
3ab	0.77 ± 0.00	1.1 ± 0.9	0.3 ± 0.21	6.2 ± 1.0
3ac	6.3 ± 2.9	6.5 ± 0.2	3.0 ± 2.0	> 10
CA-4 (1a)	0.004 ± 0.001	3.1 ± 0.2	0.37 ± 0,043	0.001 ± 0.0002

[a] IC_{50} = compound concentration required to inhibit tumor cell proliferation by 50%. Data are expressed as the mean ± SE from the dose–response curves of at least three independent experiments.

cells. The *n*-propyl derivative **3o** was half as active as **3m** and **3n** against HL-60 cells, with these latter derivatives being equipotent.

For the 2-methoxycarbonyl indole derivative **3m**, the *N*-1-methyl can be replaced with a benzyl moiety (compound **3p**) without substantial loss of activity against HeLa cells, and with a 2-fold increase in potency against HT-29 and HL-60 cells, while antiproliferative activity was reduced 2-fold against MCF-7 cells. Replacement of the C-6 methoxy of derivative **3p** with a methyl (**3l**) caused a reduction of antiproliferative activity relative to **3p**, which was moderate (2–3-fold) against three of the four cancer cell lines, and dramatic (85-fold) on HL-60 cells.

For the 2-ethoxycarbonyl-1*H*-indole derivative **3g**, replacement of hydrogen with a methyl group at the indolic nitrogen, to furnish derivative **3q**, maintained potency against HeLa and HT-29 cells relative to **3g**, while an opposite effect was observed against the other two cancer cell lines, with a 4-fold reduction of potency against MCF-7 cells and a 10-fold increase of activity against HL-60 cells.

The 3′,4′,5′-trimethoxyanilino moiety of compound **3q** can be replaced with a 3,5-dimethoxyanilino function (**3ab**) without loss of activity against HeLa and MCF-7 cells, while **3ab** was 2- and 9-fold less active than **3q** against HT-29 and HL-60 cells, respectively. The substitution of the *N*-1-methyl group of **3q** with a bulkier benzyl moiety (**3r**) was tolerated against MCF-7 and HL-60 cells, while a 2- and 3-fold reduction in activity was observed against HeLa and HT-29 cells, respectively.

Comparing the activities of derivatives characterized by the presence of a common *N*-1-methyl-5-methoxy indole nucleus and a different 2-alkoxycarbonyl function (**3m**, **3q**, **3s** and **3u**), the 2-methoxycarbonyl derivative **3m** had 2- and 3-fold reduced activity relative to the corresponding 2-ethoxycarbonyl homologue **3q** against HL-60 and HT-29 cells, while this latter compound was 2-fold less potent than **3m** against MCF-7 cells. The two derivatives showed similar potency against Hela cells. A further homologation of the alkyl chain of the alkoxycarbonyl moiety from ethyl to *n*-propyl (**3s**) slightly decreased antiproliferative activity. Reduction of activity was dramatic (two-orders of magnitude) when the *n*-propyl chain of 2-alkoxycarbonyl derivative **3s** was replaced with the isomeric, branched isopropyl group, to yield the isopropyl ester **3u**. A reduction of potency (5–10-fold) was also observed by replacing the 3,4,5-trimethoxyphenyl ring of **3s** with a 3,5-dimethoxyphenyl system (**3ac**). Replacement of the *N*-1-methyl group of *n*-propyloxycarbonyl indole derivative **3s** with a more bulky and lipophilic benzyl group (**3t**) also had a pronounced effect on potency, with a reduction in activity on three of the cell lines, while the two compounds were equipotent against HeLa cells.

For 2-methoxycarbonyl indole derivatives **3f**, **3h**, **3m**, **3p** and **3w-z**, the position of the methoxy group on the benzene portion of the indole moiety was crucial for antiproliferative activity, with the greatest potency occurring when the methoxy group was located at the C-6 position.

Comparing the activities of the three isomeric *N*-1-methyl-2-methoxycarbonyl indole derivatives **3m**, **3w** and **3z**, the greatest activity occurred when the methoxy group was located at the C-6 position (**3w**), the least when it was located at the C-7 position (**3z**).

A contrasting effect was observed comparing the activities of the *N*-1-methyl/ethyl-6-methoxy-2-methoxycarbonyl pair **3w** and **3x**, with the *N*-1-methyl derivative **3w** being 2- and 10-fold less active than its *N*-1-ethyl homologue **3x** against MCF-7 and HL-60 cells, respectively, while the two compounds were equipotent against HeLa cells. Only against the HT-29 cells, **3x** was 3-fold more active than **3w**.

For the C-6 methoxy derivative **3x**, replacement of the *N*-1-ethyl with a benzyl group (**3y**) maintained antiproliferative activity against MCF-7 and HL-60 cells, with the latter derivative being 4- and 5- fold more active than the former against Hela and HT-29 cells, respectively.

Table 2
Inhibition of tubulin polymerization and cochicine binding by compounds **3f-g**, **3k**, **3m**, **3o-p**, **3w**, **3y** and **3aa** and CA-4.

Compound	Tubulin assembly[a] IC_{50} ± SD (μM)	Colchicine binding[b] % ± SD	
		5 μM drug	0.5 μM drug
3f	0.40 ± 0.07	94 ± 0.6	53 ± 0.04
3g	0.84 ± 0.1	80 ± 2	n.d.
3k	0.53 ± 0.04	67 ± 5	n.d.
3m	0.54 ± 0.03	75 ± 2	n.d.
3o	1.6 ± 0.2	44 ± 1	n.d.
3p	> 20	15 ± 0.6	n.d.
3w	0.37 ± 0.07	97 ± 2	75 ± 4
3y	0.42 ± 0.07	68 ± 0.9	n.d.
3aa	0.47 ± 0.03	82 ± 1	n.d.
CA-4 (**1a**)	0.54 ± 0.06	98 ± 0.9	85 ± 2

n.d. = not determined.
[a] Inhibition of tubulin polymerization. Tubulin was at 10 μM.
[b] Inhibition of [^{3}H]colchicine binding. Tubulin and colchicine were at 0.5 and 5 μM concentrations, respectively.

3.2. In vitro inhibition of tubulin polymerization and colchicine binding

As presented in Table 1, nine compounds, **3f-g**, **3k**, **3m**, **3o-p**, **3w**, **3y** and **3aa**, as well as reference compound CA-4, were evaluated for their antitubulin polymerization activities in order to understand whether these new 2-alkoxycarbonyl indoles exerted their antiproliferative activities through an interaction with microtubules. The selected compounds were also examined at two different concentrations (5 and 0.5 μM) for their ability to compete with colchicine for binding to tubulin using a [^{3}H]colchicine binding assay (see Table 2).

In the tubulin polymerization assay, seven out of nine of the tested compounds (**3f-g**, **3k**, **3m**, **3aa**, **3w** and **3y**) strongly inhibited tubulin assembly with activities comparable or slightly superior (IC_{50}: 0.37–0.68 μM) to that of CA-4 (IC_{50}: 0.54 μM), while derivative **3o** (IC_{50}:1.6 μM) was 3-fold less active than CA-4. Despite appreciable cell growth inhibitory activity (IC_{50}: 0.36–0.77 μM) against the panel of cancer cells, compound **3p** was inactive in the tubulin polymerization assay (IC_{50} > 20 μM), indicating that this molecule may exert its antiproliferative effect by a different mechanism of action. When comparing the inhibition of tubulin polymerization versus the growth inhibitory effect, we found that the potency of these seven molecules for inhibition of tubulin assembly was comparable with the activity observed for CA-4, but they were considerably less active than CA-4 as antiproliferative agents against HeLa and HL-60 cells. This discrepancy can possibly be rationalized by a limited penetration into the cells or any other mechanism limiting the accessibility of these molecules to cellular tubulin.

In the colchicine competition experiments, compounds **3f-g**, **3m**, **3w** and **3aa** at 5 μM strongly inhibited [^{3}H]colchicine binding to tubulin, with 68–97% inhibition. Compounds **3f** and **3w** were the most potent inhibitors of tubulin polymerization (IC_{50} = 0.40 and 0.37 μM, respectively), and this was also confirmed in the colchicine binding assay (94% and 97% inhibition at 5 μM). When the concentration of **3f** and **3w** was 0.5 μM, 53% and 75% inhibition, respectively, of the binding of [^{3}H]colchicine to tubulin was observed. In addition, compounds **3f** and **3w** were as active as CA-4 as inhibitors of colchicine binding at 5 μM, while the difference between **3f** and CA-4 was more prominent than that between **3w** and CA-4 at 0.5 μM.

Comparing the activities of compounds **3m** and **3aa**, we can observe that the 3′,4′,5′-trimethoxyphenyl moiety of **3m**, a well-defined pharmacophore for the inhibition of tubulin polymerization found in colchicine, CA-4 and podophyllotoxin, was not essential for potent inhibition of tubulin polymerization and colchicine binding. This moiety can be replaced with the 3′,5′-dimethoxyphenyl ring of derivative **3aa** without loss of activity (IC_{50} = 0.54 and 0.47 μM for assembly, 75% and 82% inhibition of the binding of colchicine for **3m** and **3aa**, respectively, at 5 μM). A linear correlation between inhibition of tubulin assembly and colchicine binding inhibition was observed between analogue pairs **3m**/**3aa** and **3f**/**3w**, while a different behavior was observed for derivatives **3w** and **3y**. These latter compounds were both equipotent as inhibitors of tubulin assembly, while **3w** was much more active than **3y** as an inhibitor of [^{3}H]colchicine binding (97% and 68% inhibition, respectively).

3.3. Molecular modeling studies

The tubulin colchicine site is a flexible area, which can adapt to different ligands by changing the architecture of the pocket. Diverse ligands may induce different conformations of the same protein, and therefore an inhibitor, whose structure induces a specific protein conformation, may not be correctly docked by the program against another protein conformation, often giving poor correlation between biological data and computational results. In order to explore the potential binding mode of selected newly synthesized compounds (**3f**, **3g**, **3k**, **3m**, **3o**, **3p**, **3w**, **3y** and **3aa**) and to consider the flexibility of the colchicine binding domain, an ensemble docking study using Glide SP was performed [40]. Ensemble docking reduces potential evaluation errors associated with receptor rigidity by docking a series of ligands against multiple crystal structures of the same protein.

Three crystal structures were used: tubulin co-crystallized with vinblastine (PDB ID: 5BMV) [41], in which the colchicine binding domain is unoccupied; tubulin co-crystallized with colchicine (PDB ID: 4O2B) [42]; and tubulin co-crystallized with microtubule-destabilizing CA-4 (**1a**) (PDB ID: 5LYJ) [43]. These crystals represent three different conformations of the colchicine binding area.

While, as expected, none of the molecules was docked by Glide in the unbound form of tubulin (5BMV), the CA-4-tubulin complex (5LYJ) was able to correctly accommodate only compound **3f** and **3g**, the unsubstituted derivatives at the *N*-1 position, whereas the rest of the molecules either provided an implausible binding mode if correlated with their biological activity (**3k**, **3m**, **3o** and **3aa**), or were not docked by the program (**3p**, **3w**, and **3y**). These compounds are all characterised by various substitutions at the *N*-1 position of the indole ring. In contrast, all the compounds were correctly docked in the colchicine-tubulin crystal structure (4O2B). The loop formed by residues between βGln247 and βAla250 occupies the central area of the colchicine domain on the unoccupied tubulin structure, not allowing the binding of any ligand (Fig. 2). The presence of colchicine or CA-4 forces this loop to move away from this area, inducing the formation of the binding pocket. A second loop, which goes from αSer178 to αVal181, further reduces the size of the colchicine domain by moving toward the β-tubulin unit in two of the crystal structures, the unbound form (5BMV) and the CA-4-tubulin complex (5LYJ), whereas, in the third crystal structure (4O2B), the lateral amide substituent of colchicine pushes this loop to widen the binding area (Fig. 2).

3f and **3g**, the two compounds that obtained the best docking score in both crystals, occupy the active site similarly to the co-crystallized ligands, with the trimethoxyphenyl ring overlapping the same ring in the CA-4 and colchicine structures (Fig. 3).

The anilinic nitrogen bridging the indole nucleus and the 3′,4′,5′-trimethoxyphenyl confers a conformation to the molecules that mimics the CA-4 *cis*-olefin bridge and the central colchicine B ring. H-bond formation between the 4-methoxy group and βCys241 is present in both crystals, while interaction between the indole NH and αThr179 and between the carboxylic group and βAla250/βAsn268 further stabilize the compounds on the CA-4 binding site. As mentioned above, introduction of various substitutions at the *N*-1 position of the indole ring does not allow a correct occupation of the binding area on the CA-4-tubulin complex (5LYJ), potentially due to steric clashes between the different substituents and the αSer178-αVal181 loop. Analyzing the

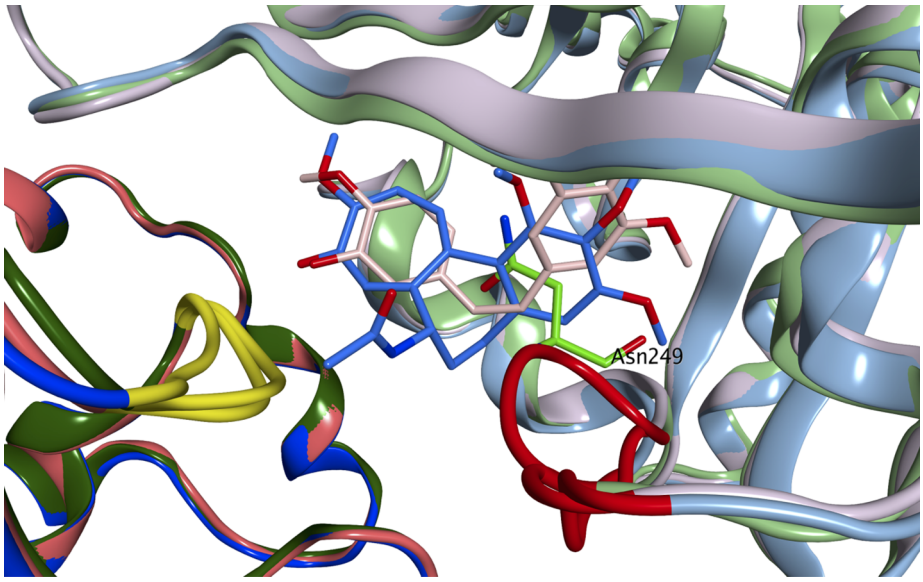

Fig. 2. Superposition of the colchicine site of three tubulin crystal structures: unoccupied colchicine binding domain (PDB ID: 5BMV). The β-tubulin unit is represented as a light green ribbon; the α-tubulin unit is represented as a dark green ribbon; tubulin co-crystallized with colchicine (PDB ID: 4O2B). The β-tubulin unit is represented as an air force blue ribbon; the α-tubulin unit is represented as a dark blue ribbon. Co-crystallized colchicine is shown in blue; tubulin co-crystallized with microtubule-destabilizing CA-4 (PDB ID: 5LYJ). The β-tubulin unit is represented as a pink ribbon; the α-tubulin unit is represented as a salmon ribbon. Co-crystallized CA-4 is shown in pink). The βGln247-βAla250 loop is represented in red, whereas the αSer178-αVal181 loop in represented in yellow. Note the different architecture of the colchicine binding area in the three crystal structures.

docking results on the colchicine-tubulin crystal structure (4O2B), the simultaneous presence of the methoxy group at the 5-position and a substituent at the *N*-1 of the indole nucleus forces the compounds to occupy the active site in a non-optimal manner, potentially resulting in a reduced inhibition of colchicine binding (Fig. 4). In particular, the anilinic nitrogen bridge assumes a conformation that impedes the central indole core from overlapping the central colchicine B ring, and this effect is accentuated with increasing *N*-1 substituent size. **3p**, with a benzyl substituent at *N*-1, did not have a plausible binding mode, in agreement with its low ability to inhibit colchicine binding (Fig. 4).

Moving the methoxy group from position 5 to 6 (**3w**) allows a correct occupation of the binding area, comparable to the binding pose found for **3f**, and is in accord with the colchicine binding assay results (Fig. 5). Increasing the size of the *N*-1 substituent to a benzyl ring (**3y**) causes a change in the anilinic nitrogen bridge similar to the one observed for **3m**, potentially explaining the similar inhibition of colchicine binding found for these three compounds (Fig. 5). Finally, the 3′,5′-dimethoxyphenyl compound **3aa** binds in the active site similarly to the 3′,4′,5′-trimethoxyphenyl derivative **3m**, in accord with their similar inhibition of colchicine binding.

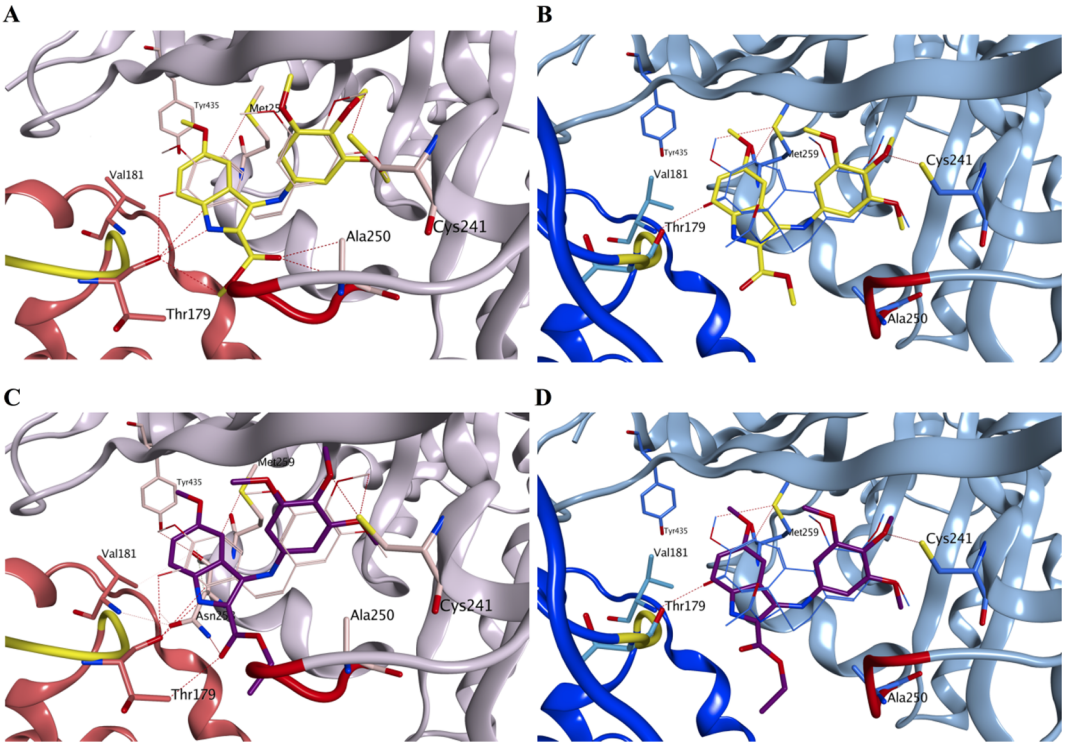

Fig. 3. Proposed binding mode for compound **3f** in 5LYJ (**A**) and 4O2B (**B**) and for compound **3g** in 5LYJ (**C**) and 4O2B (**D**). The two compounds occupy the active site similarly to the co-crystallized ligands, especially their trimethoxyphenyl rings. Co-crystallized CA-4 is shown in pink, colchicine in blue, compound **3f** in yellow and compound **3g** in dark purple. The β-tubulin unit from 5LYJ is represented as a pink ribbon, and the α-tubulin unit is shown as a salmon ribbon. The β-tubulin unit from 4O2B is represented as a blue ribbon, and the α-tubulin unit is represented as a dark blue ribbon. The βGln247-βAla250 loop is represented in red, and the αSer178-αVal181 loop in represented in yellow.

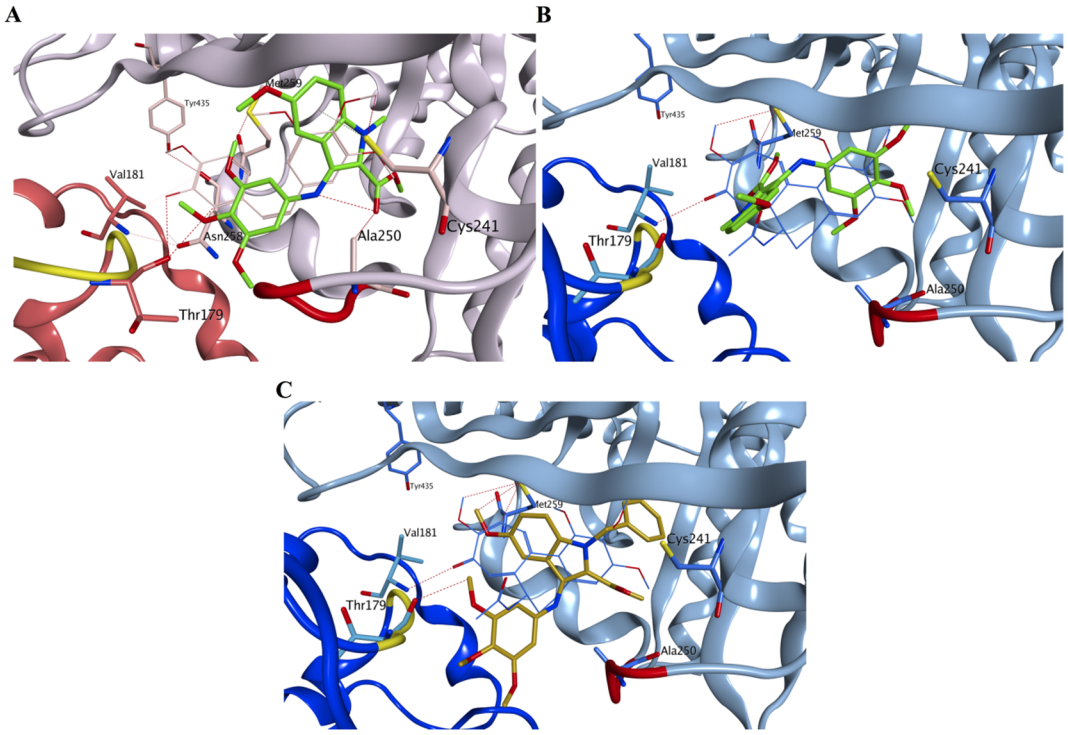

Fig. 4. Proposed binding modes for compound **3m** in 5LYJ (**A**) and 4O2B (**B**) and for compound **3p** in 4O2B (**C**). Introduction of a methyl group at the *N*-1 position of the indole ring does not allow correct occupation of the binding area on the CA-4-tubulin complex (5LYJ) by **3m** (**A**), potentially due to steric clashes between the methyl group and the αSer178-αVal181 loop. Although compound **3m** is able to bind to the colchicine-tubulin crystal structure (4O2B), the simultaneous presence of the methoxy group at the 5-position and a substituent at the *N*-1 of the indole nucleus forces the compound to sit in the active site in a non-optimal manner (**A**). In particular, the anilinic nitrogen bridge assumes a conformation that impedes the central indole core of **3m** from superimposing on ring B of colchicine. Compound **3p**, having a benzyl substituent on *N*-1, did not show a plausible binding mode on 4O2B, which is consistent with its minimal inhibition of colchicine binding. Co-crystallized CA-4 is shown in pink, colchicine in blue, compound **3m** in green and compound **3p** in gold. The β-tubulin unit from 5LYJ is represented as a pink ribbon, and the α-tubulin unit is shown as a salmon ribbon. The β-tubulin unit from 4O2B is represented as a blue ribbon, and the α-tubulin unit is represented as a dark blue ribbon. The βGln247-βAla250 loop is represented in red, and the αSer178-αVal181 loop in represented in yellow.

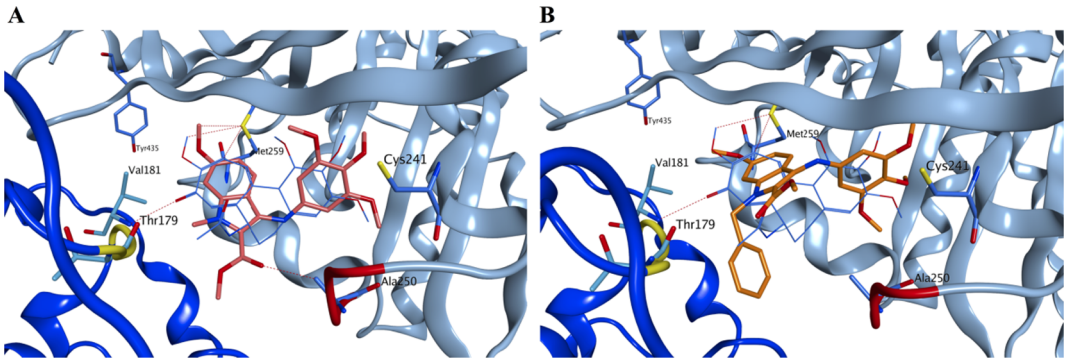

Fig. 5. Proposed binding mode for compounds **3w** (**A**) and **3y** (**B**) in 4O2B. Moving the methoxy group from position 5 to 6 in **3w** allows a correct occupation of the binding area despite the presence of a methyl group at the *N*-1 position (**A**). Increasing the size of the *N*-1 substituent to a benzyl ring in **3y** causes a change in the anilinic nitrogen bridge similar to the one observed for **3m.** Co-crystallized colchicine is shown in blue, compound **3w** in salmon and compound **3y** in orange. The β-tubulin unit from 4O2B is represented as a blue ribbon, and the α-tubulin unit is represented as a dark blue ribbon. The βGln247-βAla250 loop is represented in red, and the αSer178-αVal181 loop in represented in yellow.

In conclusion, molecular docking studies have given important insights into the potential binding mode for this family of compounds. Furthermore, the results have highlighted the importance of selecting the appropriate crystal structure of a given protein to perform reliable docking simulations.

3.4. Analysis of cell cycle effects

Since molecules exhibiting activity on tubulin binding should cause alteration of cell cycle parameters, leading to a preferential G2/M blockade, the effects of compounds **3m**, **3w** and **3y** on cell cycle distribution were analyzed on HeLa cells cultured for 24 h in the presence of. six different concentrations ranging from 6.4×10^{-4} to 2 μM for each tested derivative (Table 3). All three compounds caused a dose-dependent accumulation of cells in the G2/M phase, with a concomitant reduction of cells in the G1 phase. Compound **3w** was the most active compound since at 0.0032 μM it induced a significant increase in cells in the G2/M phase (Fig. 6), in excellent agreement with the data on inhibition of tubulin polymerization. The other two compounds (**3m** and **3y**) were less potent and were similar to each other, blocking the

Table 3
Cell cycle analysis of compounds **3m, 3w, 3y** and reference compound CA-4 (**1a**).

Compound	Concentration (μM)	Distribution of cells (%)[a]			
		Sub-G_1	G_0/G_1	S	G_2/M
3m	2	9.95 ± 4.11	12.22 ± 4.34	12.01 ± 4.39	65.82 ± 4.57
	0.4	11.62 ± 1.31	16.46 ± 2.91	16.50 ± 4.69	55.42 ± 8.79
	0.08	6.18 ± 1.44	25.94 ± 2.39	37.23 ± 6.27	30.66 ± 9.54
	0.016	1.75 ± 1.23	58.74 ± 11.27	16.90 ± 1.17	22.60 ± 8.88
	0.0032	2.78 ± 2.99	65.21 ± 3.57	17.68 ± 0.41	14.33 ± 5.31
	0.00064	4.19 ± 2.90	61.99 ± 1.65	19.59 ± 2.28	14.22 ± 4.03
	0	3.22 ± 3.45	61.93 ± 4.18	14.59 ± 2.02	18.99 ± 3.83
3w	2	7.99 ± 5.49	8.74 ± 1.33	11.46 ± 1.18	71.80 ± 4.83
	0.4	7.21 ± 2.26	12.87 ± 5.06	14.13 ± 5.06	65.80 ± 5.25
	0.08	5.99 ± 2.14	10.57 ± 2.52	13.80 ± 1.69	69.66 ± 1.94
	0.016	5.59 ± 3.30	10.23 ± 2.78	13.63 ± 4.68	70.55 ± 10.62
	0.0032	6.76 ± 1.61	14.93 ± 3.14	33.04 ± 4.12	45.27 ± 3.77
	0.00064	3.14 ± 2.17	67.28 ± 4.13	15.60 ± 3.80	13.98 ± 2.04
	0	3.22 ± 3.45	61.93 ± 4.18	14.59 ± 2.02	18.99 ± 3.83
3y	2	7.97 ± 2.47	10.42 ± 5.67	11.01 ± 2.81	70.61 ± 5.64
	0.4	9.33 ± 2.45	11.51 ± 3.82	12.42 ± 2.62	66.75 ± 4.77
	0.08	4.46 ± 0.45	52.79 ± 3.93	18.69 ± 1.67	24.05 ± 3.13
	0.016	3.60 ± 2.34	67.42 ± 4.08	20.77 ± 4.73	8.21 ± 5.60
	0.0032	11.12 ± 12.37	59.46 ± 10.66	21.89 ± 0.89	7.54 ± 3.03
	0.00064	13.78 ± 13.85	60.32 ± 12.40	20.71 ± 5.26	5.19 ± 1.39
	0	3.22 ± 3.45	61.93 ± 4.18	14.59 ± 2.02	18.99 ± 3.83
CA-4 (**1a**)	2	14.75 ± 6.47	8.45 ± 4.23	7.74 ± 0.54	69.07 ± 4.36
	0.4	8.13 ± 3.97	10.55 ± 3.80	14.32 ± 2.86	66.99 ± 4.98
	0.08	6.78 ± 2.80	10.10 ± 2.49	15.19 ± 1.83	67.92 ± 6.91
	0.016	9.32 ± 1.12	14.31 ± 2.87	15.24 ± 3.07	61.13 ± 1.31
	0.0032	13.63 ± 4.85	13.90 ± 4.10	15.43 ± 0.93	57.02 ± 9.27
	0.00064	10.50 ± 2.60	33.98 ± 11.03	23.41 ± 10.42	32.11 ± 1.54
	0	3.22 ± 3.45	61.93 ± 4.18	14.59 ± 2.02	18.99 ± 3.83

[a] Percentages of cells in each phase of the cell cycle in HeLa cells treated with the indicated compounds at the indicated concentrations for 24 h. CA-4 (**1a**) was used as a positive control. Cells were fixed and labeled with DAPI and analyzed by high content imaging as described in the experimental section. Data are expressed as the mean ± SD of two independent experiments.

cell cycle only at 0.08 μM.

*3.5. Apoptosis induction assay of compounds **3m, 3w** and **3y** in HeLa cancer and human non-cancer cells*

To determine the ability of compounds **3m**, **3w** and **3y** to induce apoptosis, HeLa and healthy human peripheral blood mononuclear cells (PBMC) were incubated and monitored at 37 °C for three days in the presence of each compound at different concentrations ranging from 6.4×10^{-4} to 10 μM. The induction of apoptosis was monitored by the activation of caspase 3/7, a well-known marker of apoptosis, using a commercial kit, as described in the experimental procedures. CA-4 was

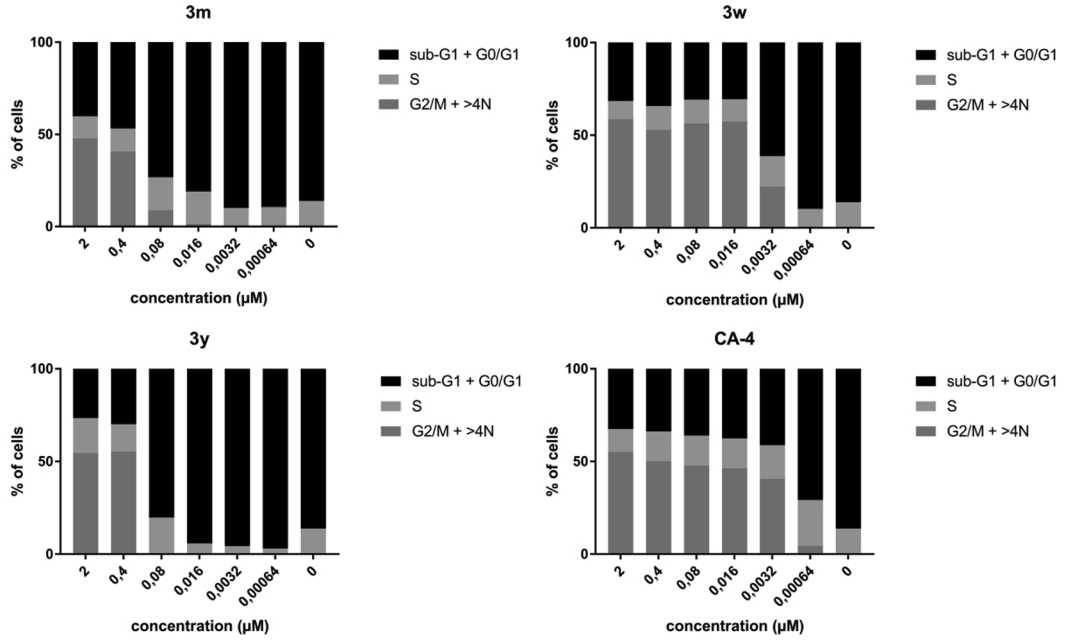

Fig. 6. The impact of compounds **3m**, **3w** and **3y** on cell cycle of HeLa cells. HeLa cells were treated with six different concentrations of **3m**, **3w**, **3y** and reference compound CA-4 (**1a**) for 24 h and then assayed via high content imaging. The bar chart shows the percentage of cell cycle distribution based on the imaging results.

Table 4
EC_{50} values for apoptosis induction by **3m**, **3w**, **3y** and control compound CA-4 (**1a**) in HeLa cancer cells and PBMC.

	EC_{50}[a] (μM) caspase 3/7 activation	
Compound	HeLa	PBMC
3m	0.37 ± 0.11	> 10
3w	0.069 ± 0.008	> 10
3y	0.53 ± 0.16	> 10
CA-4 (1a)	0.005 ± 0.002	> 10

[a] EC_{50} = compound concentration required to activate caspase 3/7 by 50%. Data are expressed as the mean ± SE from the dose–response curves of at least two independent experiments.

employed as a control compound. As shown in Table 4, derivatives **3m**, **3w** and **3y**, as well as CA-4, were ineffective in PBMC, with IC_{50} values (> 10 μM) that were negligible as compared with those found against the HeLa cancer cells and against other cancer cell lines (Table 1). Altogether, these data suggest that these compounds not only induce apoptosis but may also have cancer cell selective antiproliferative properties.

4. Conclusions

In this report we have demonstrated that replacing the sulfur atom, carbonyl moiety or methylene unit bridging the 3′,4′,5′-trimethoxyphenyl ring and C-3 position of the indole nucleus of compounds with general structure **2** previously reported by Silvestri *et al.* with an anilinic nitrogen (NH) yielded a new series of 2-alkoxycarbonyl-3-anilino indoles with general formula **3** with potent antiproliferative activity caused by their inhibition of tubulin polymerization. Various substituents were tolerated on the indolic nitrogen, with alkyl and benzyl substitution of compounds **3k-ac** that generally led to little effect on antiproliferative potency, while a small-sized methoxy/ethoxycarbonyl moiety at the 2-position of the indole nucleus is important for optimal antiproliferative activity (as depicted in Fig. 7). The 3′,4′,5′-trimethoxyanilino moiety at the 3-position of the indole skeleton can be replaced by a 3′,5′-dimethoxyanilino function without a loss of activity (compare **3a** with **3i**, **3b** with **3j**, **3m** with **3aa** and **3q** with **3ab**). Further analysis of the SAR showed that antiproliferative activity is also related to the presence and position of the methoxy group at the C-5 or C-6 position on the benzene portion of the indole ring, with the 6-OMe derivatives generally more active than their corresponding 5-OMe counterparts (i.e, **3g** *vs.* **3h**, **3m** *vs.* **3w**, **3n** *vs.* **3x**, **3p** *vs.* **3y**).

The data identified tubulin as the molecular target of most compounds, since those with the greatest inhibitory effects on cell growth strongly inhibited tubulin assembly and the binding of colchicine to tubulin, with a good correlation between the inhibition of tubulin polymerization versus the antiproliferative effects. In particular, we have identified 2-methoxycarbonyl-3-(3′,4′.5′-trimethoxyanilino)-5-methoxyindole (**3f**) and 1-methyl-2-methoxycarbonyl-3-(3′,4′,5′-trimethoxyanilino)-6-methoxyindole (**3w**) as new antiproliferative agents that target tubulin at the colchicine site with antitubulin activities comparable to that of the reference compound CA-4.

Three of the most active compounds in the tubulin assay, corresponding to 2-methoxycarbonyl-3-(3′,4′.5′-trimethoxyanilino) indoles **3w**, **3m** and **3y**, induced arrest of Hela cells in the G2/M phase of the cell cycle. Further experiments demonstrated that these compounds induce apoptosis in Hela cells and were practically devoid of significant apoptotic activity in normal PBMCs.

5. Experimental protocols

5.1. Chemistry

5.1.1. Materials and methods

^1H experiments were recorded on either a Bruker AC 200 or a Varian 400 Mercury Plus spectrometer, while ^{13}C NMR spectra were recorded on a Varian 400 Mercury Plus spectrometer. Chemical shifts (δ) are given in ppm upfield from tetramethylsilane as internal standard, and the spectra were recorded in appropriate deuterated solvents, as indicated. Positive-ion electrospray ionization (ESI) mass spectra were recorded on a double-focusing Finnigan MAT 95 instrument with BE geometry. Melting points (mp) were determined on a Buchi-Tottoli apparatus and are uncorrected. All products reported showed ^1H and ^{13}C NMR spectra in agreement with the assigned structures. The purity of tested compounds was determined by combustion elemental analyses conducted by the Microanalytical Laboratory of the Chemistry Department of the University of Ferrara with a Yanagimoto MT-5 CHN recorder elemental analyzer. All tested compounds yielded data consistent with a purity of at least 95% as compared with the theoretical values. All reactions were carried out under an inert atmosphere of dry nitrogen, unless otherwise indicated. Standard syringe techniques were used for transferring dry solvents. Reaction courses and product mixtures were routinely monitored by TLC on silica gel (precoated F_{254} Merck plates), and compounds were visualized with aqueous $KMnO_4$. Flash chromatography was performed using 230–400 mesh silica gel and the indicated solvent system. Organic solutions were dried over anhydrous Na_2SO_4.

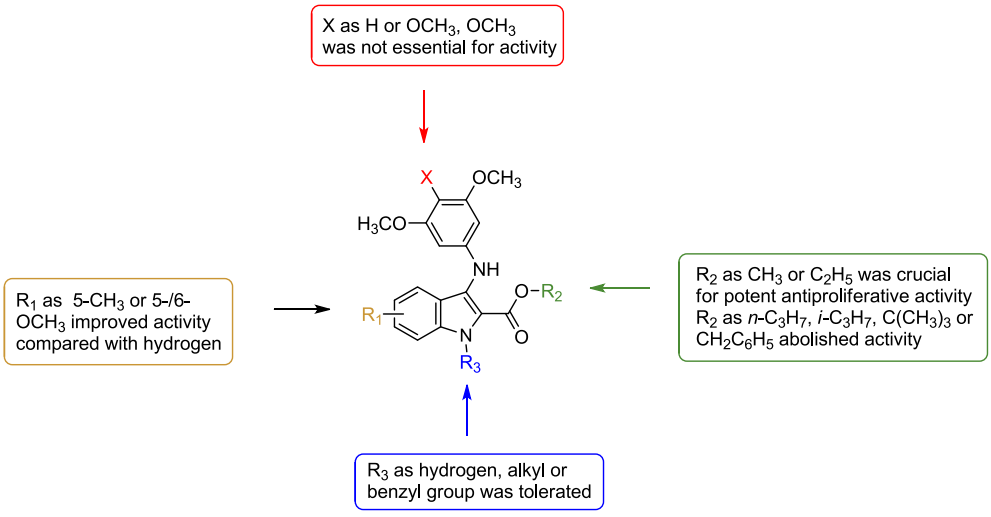

Fig. 7. SAR analysis of 2-alkoxycarbonyl-3-anilino indole analogues **3a-c.**

*5.1.2. General method A for the synthesis of compounds **7a-h***

A suspension of the appropriate 2-aminobenzonitrile **6a-d** (10 mmol), appropriate alkyl or benzyl bromoacetate (10 mmol) and $NaHCO_3$ (0.99 g, 12 mmol, 1.2 equiv.) in the appropriate solvent (10 mL) was stirred at reflux for 24 h. After this time, the appropriate alkyl or benzyl bromoacetate (10 mmol) was added and the mixture heated at reflux for an additional 24 h. The reaction mixture was cooled to ambient temperature and filtered through Celite, then the filtrate was evaporated *in vacuo*. The residue was diluted with dichloromethane (25 mL) and washed sequentially with water (10 mL) and brine (10 mL). The organic layer was dried over Na_2SO_4, filtered and concentrated under reduced pressure, and the residue was stirred with the appropriate solvent or purified by flash column chromatography on silica gel.

*5.1.2.1. Methyl 2-[(2-cyanophenyl)amino]acetate (**7a**)*. Following general procedure A, the product was synthesized using 2-aminobenzonitrile **6a**, methyl bromoacetate and MeOH as solvent. The crude residue was suspended in EtOH and filtered to furnish **7a** as a yellow solid. Yield: 54%, mp 86 °C. ^{1}H NMR ($CDCl_3$) δ: 3.80 (s, 3H), 3.99 (d, J = 5.4 Hz, 2H), 5.12 (bs, 1H), 6.53 (d, J = 8.4 Hz, 1H), 6.75 (t, J = 8.4 Hz, 1H), 7.42 (m, 2H). MS (ESI): $[M]^+$ = 190.5.

*5.1.2.2. Ethyl 2-[(2-cyanophenyl)amino]acetate (**7b**)*. Following general procedure A, the product was synthesized using 2-aminobenzonitrile **6a**, ethyl bromoacetate and EtOH as solvent. The crude residue was suspended in petroleum ether and filtered to furnish **7b** as a yellow solid. Yield: 83%, mp 90 °C. ^{1}H NMR ($CDCl_3$) δ: 1.30 (t, J = 7.2 Hz, 3H), 3.97 (d, J = 5.4 Hz, 2H), 4.25 (q, J = 7.2 Hz, 2H), 5.22 (bs, 1H), 6.53 (d, J = 8.2 Hz, 1H), 6.74 (t, J = 8.2 Hz, 1H), 7.41 (m, 2H). MS (ESI): $[M+1]^+$ = 205.3.

*5.1.2.3. tert-butyl 2-[(2-cyanophenyl)amino]acetate (**7c**)*. Following general procedure A, the product was synthesized using 2-aminobenzonitrile **6a**, *tert*-butyl bromoacetate and *tert*-butanol as solvent. The crude residue was purified by flash chromatography, using ethyl acetate:petroleum ether 1:9 (v:v) as eluent, to furnish **7c** as a yellow oil. Yield: 52%. ^{1}H NMR ($CDCl_3$) δ: 1.48 (s, 9H), 3.88 (d, J = 5.0 Hz, 2H), 5.21 (bs, 1H), 6.51 (d, J = 8.2 Hz, 1H), 6.73 (t, J = 8.2 Hz, 1H), 7.40 (m, 2H). MS (ESI): $[M]^+$ = 233.3.

*5.1.2.4. Benzyl 2-[(2-cyanophenyl)amino]acetate (**7d**)*. Following general procedure A, the product was synthesized using 2-aminobenzonitrile **6a**, benzyl bromoacetate and acetonitrile as solvent. The crude residue was purified by flash chromatography, using ethyl acetate:petroleum ether 1:9 (v:v) as eluent, to furnish **7d** as a white solid. Yield: 77%, mp 92 °C. ^{1}H NMR ($CDCl_3$) δ: 4.02 (d, J = 5.6 Hz, 2H), 5.12 (bs, 1H), 5.23 (s, 2H), 6.50 (d, J = 8.4 Hz, 1H), 6.74 (t, J = 8.4 Hz, 1H), 7.36 (m, 7H). MS (ESI): $[M]^+$ = 266.3.

*5.1.2.5. Ethyl 2-[(5-chloro-2-cyanophenyl)amino]acetate (**7e**)*. Following general procedure A, the product was synthesized using 4-chloro-2-aminobenzonitrile **6b**, ethyl bromoacetate and DMF as solvent. The crude residue was purified by flash chromatography, using ethyl acetate:petroleum ether 1:9 (v:v) as eluent, to furnish **7e** as a white solid. Yield: 77%, mp 132 °C. ^{1}H NMR ($CDCl_3$) δ: 1.34 (t, J = 7.0 Hz, 3H), 3.94 (d, J = 5.4 Hz, 2H), 4.26 (q, J = 7.2 Hz, 2H), 5.20 (bs, 1H), 7.07 (dd, J = 8.2 and 2.0 Hz, 1H), 7.45 (d, J = 8.2 Hz, 1H), 8.36 (d, J = 2.0 Hz, 1H). MS (ESI): $[M+1]^+$ = 239.7.4.

*5.1.2.6. Methyl 2-[(2-cyano-4-methoxyphenyl)amino]acetate (**7f**)*. Following general procedure A, the product was synthesized using 5-methoxy-2-aminobenzonitrile **6c**, methyl bromoacetate and CH_3CN as solvent. The crude residue was purified by flash chromatography, using ethyl acetate:petroleum ether 3:7 (v:v) as eluent, to furnish **7f** as a white solid. Yield: 58%, mp 132 °C. ^{1}H NMR ($CDCl_3$) δ: 3.89 (m, 5H), 4.08 (s, 3H), 5.16 (bs, 2H), 6.62 (dd, J = 9.0 and 2.2 Hz, 1H), 7.53 (d, J = 9.0 Hz, 1H), 7.93 (d, J = 2.2 Hz, 1H). MS (ESI): $[M]^+$ = 221.4.

*5.1.2.7. Ethyl 2-[(2-cyano-4-methoxyphenyl)amino]acetate (**7g**)*. Following general procedure A, the product was synthesized using 5-methoxy-2-aminobenzonitrile **6c**, ethyl bromoacetate and CH_3CN as solvent. The crude residue was purified by flash chromatography, using ethyl acetate:petroleum ether 3:7 (v:v) as eluent, to furnish **7g** as a white solid. Yield: 56%, mp 124 °C. ^{1}H NMR ($CDCl_3$) δ: 1.34 (t, J = 7.2 Hz, 3H), 3.88 (d, J = 5.2 Hz, 2H), 3.96 (s, 3H), 4.24 (q, J = 7.2 Hz, 2H), 5.22 (bs, 1H), 6.59 (dd, J = 9.0 and 2.4 Hz, 1H), 7.18 (bs, 1H), 7.41 (d, J = 9.0 Hz, 1H), 7.87 (d, J = 2.4 Hz, 1H). MS (ESI): $[M]^+$ = 235.2.

*5.1.2.8. Methyl 2-[(2-cyano-5-methoxyphenyl)amino]acetate (**7h**)*. Following general procedure A, the product was synthesized using 4-methoxy-2-aminobenzonitrile **6d**, methyl bromoacetate and CH_3CN as solvent. The crude residue was purified by flash chromatography, using ethyl acetate:petroleum ether 3:7 (v:v) as eluent, to furnish **7h** as a white solid. Yield: 58%, mp 132 °C. 3.89 (m, 5H), 4.10 (s, 3H), 5.06 (bs, 1H), 6.59 (dd, J = 8.8 and 2.4 Hz, 1H), 7.18 (bs, 1H), 7.41 (d, J = 8.8 Hz, 1H), 7.87 (d, J = 2.4 Hz, 1H). MS (ESI): $[M]^+$ = 221.4

*5.1.3. General method B for the preparation of compounds **8a-h***

Potassium *tert*-butoxide (0.56 g, 5 mmol) was dissolved in dry THF (5 mL). The mixture was cooled in a bath of ice and water, and the appropriate alkyl/benzyl 2-((2-cyanophenyl)amino)acetate **7a-h** (5 mmol) dissolved in THF (5 mL) was added dropwise. The reaction mixture was allowed to warm to room temperature, stirred for 2 h and diluted with water (10 mL). The mixture was extracted with EtOAc (20 mL) and the organic layer washed with a water and brine solution. The EtOAc layer was dried over Na_2SO_4 and evaporated to obtain a residue purified by flash column chromatography on silica gel. For the characterization of methyl 3-amino-1*H*-indole-2-carboxylate (**8a**), ethyl 3-amino-1*H*-indole-2-carboxylate (**8b**) and *tert*-butyl-3-amino-1*H*-indole-2-carboxylate (**8c**), see reference [44]. For the characterization of ethyl 3-amino-5-methoxy-1*H*-indole-2-carboxylate (**8g**) and methyl 3-amino-6-methoxy-1*H*-indole-2-carboxylate (**8h**), see references [45] and [46], respectively.

*5.1.3.1. Benzyl 3-amino-1H-indole-2-carboxylate (**8d**)*. Following general procedure B, the crude residue was purified by flash chromatography, using ethyl acetate:petroleum ether 3:7 (v:v) as eluent, to furnish **8d** as an eggshell solid. Yield: 54%, mp 112 °C. ^{1}H NMR ($CDCl_3$) δ: 4.72 (bs, 2H), 5.37 (s, 2H), 7.12 (m, 1H), 7.37 (m, 7H), 7.56 (d, J = 7.2 Hz, 1H), 7.82 (bs, 1H). MS (ESI): $[M]^+$ = 267.3.

*5.1.3.2. Ethyl 3-amino-6-chloro-1H-indole-2-carboxylate (**8e**)*. Following general procedure B, the crude residue was purified by flash chromatography, using ethyl acetate:petroleum ether 3:7 (v:v) as eluent, to furnish **8e** as a brown solid. Yield: 65%, mp 168 °C. ^{1}H NMR ($CDCl_3$) δ: 1.37 (t, J = 7.4 Hz, 3H), 4.34 (q, J = 7.4 Hz, 2H), 4.82 (bs, 2H), 6.98 (dd, J = 8.6 and 2.0 Hz, 1H), 7.26 (s, 1H), 7.44 (d, J = 8.6 Hz, 1H), 7.82 (bs, 1H). MS (ESI): $[M]^+$ = 239.7.

*5.1.3.3. Methyl 3-amino-5-methoxy-1H-indole-2-carboxylate (**8f**)*. Following general procedure B, the crude residue was purified by flash chromatography, using ethyl acetate:petroleum ether 1:1 (v:v) as eluent, to furnish **8f** as a brown solid. Yield: 63%, mp 161 °C. ^{1}H NMR (DMSO-d_6) δ: 3.83 (s, 3H), 3.96 (s 3H), 4.44 (bs, 2H), 6.93 (d, J = 2.4 Hz, 1H), 7.05 (dd, J = 9.0 and 2.4 Hz, 1H), 7.57 (d, J = 9.0 Hz, 1H), 7.31 (d, J = 9.0 Hz, 1H), 11.8 (bs, 1H). MS (ESI): $[M]^+$ = 221.3.

*5.1.4. General method C for the synthesis of compounds **10a-g***

To a solution of the appropriate 2-alkoxycarbonyl-1*H*-indole derivative **9a-g** (2 mmol) in DMF (20 mL) cooled to 0 °C was added dropwise a mixture of NBS (0.43 g, 2.4 mmol) in DMF (10 mL), and the

resulting mixture was stirred for 1 h. The mixture was then diluted with cold water (30 mL) and extracted with dichloromethane (2 × 20 mL). The combined organics were washed with water (3 × 20 mL), brine (20 mL), dried (Na_2SO_4) and evaporated to give a solid, which was purified by crystallization with the appropriate solvent or purified by flash chromatography on silica gel.

*5.1.4.1. Methyl 3-bromo-5-methyl-1H-indole-2-carboxylate (**10a**).* Following general procedure C, the crude residue purified by flash chromatography using ethyl acetate:petroleum ether 1:9 (v:v) as eluent furnished **10a** as a white solid. Yield: 77%, mp 162–164 °C. ^{1}H NMR (DMSO-d_6) δ: 2.40 (s, 3H), 3.89 (s, 3H), 7.16 (dd, J = 8.6 and 1.2 Hz, 1H), 7.31 (d, J = 8.6 Hz, 1H), 7.39 (d, J = 1.2 Hz, 1H), 12.2 (s, 1H). MS (ESI): $[M]^+$ = 268.1, 270.2.

*5.1.4.2. Methyl 3-bromo-5-methoxy-1H-indole-2-carboxylate (**10b**).* Following general procedure C, petroleum ether was added to the residue, the mixture stirred for 15 min, and the resulting precipitate was collected by filtration to furnish the title compound **10b** as a brown solid (> 95% yield); mp 173–174 °C. ^{1}H NMR (DMSO-d_6) δ: 3.85 (s, 3H), 3.89 (s, 3H), 6.89 (d, J = 2.2 Hz, 1H), 6.97 (dd, J = 8.8 and 2.2 Hz, 1H), 7.36 (d, J = 8.8 Hz, 1H), 12.2 (bs, 1H). MS (ESI): $[M]^+$ = 284.1, 286.2.

*5.1.4.3. Ethyl 3-bromo-5-methoxy-1H-indole-2-carboxylate (**10c**).* Following general procedure C, the crude residue purified by flash chromatography using ethyl acetate:petroleum ether 3:7 (v:v) as eluent furnished **10c** as a white solid. Yield: 89%, mp 134–136 °C. ^{1}H NMR (DMSO-d_6) δ: 1.36 (t, J = 7.0 Hz, 3H), 3.81 (s, 3H), 4.31 (q, J = 7.0 Hz, 2H), 6.89 (d, J = 2.4 Hz, 1H), 6.97 (d, J = 9.0 and 2.4 Hz, 1H), 7.37 (d, J = 9.0 Hz, 1H), 12.1 (s, 1H). MS (ESI): $[M]^+$ = 298.1, 300.1.

*5.1.4.4. n-Propyl 3-bromo-5-methoxy-1H-indole-2-carboxylate (**10d**).* Following general procedure C, the crude residue purified by flash chromatography using ethyl acetate:petroleum ether 1:9 (v:v) as eluent furnished **10d** as a white solid. Yield: 75%, mp 146–148 °C. ^{1}H NMR (DMSO-d_6) δ: 1.03 (t, J = 7.4 Hz, 3H), 1.74 (m, 2H), 3.81 (s, 3H), 4.28 (t, J = 7.4 Hz, 2H), 6.89 (dd, J = 2.2 Hz, 1H), 6.97 (d, J = 9.0 and 2.2 Hz, 1H), 7.37 (d, J = 9.0 Hz, 1H), 12.1 (s, 1H). MS (ESI): $[M]^+$ = 312.2, 314.3.

*5.1.4.5. Isopropyl 3-bromo-5-methoxy-1H-indole-2-carboxylate (**10e**).* Following general procedure C, the crude residue purified by flash chromatography using ethyl acetate:petroleum ether 1:9 (v:v) as eluent furnished **10e** as a white solid. Yield: 75%, mp 178–179 °C. ^{1}H NMR (DMSO-d_6) δ: 1.33 (d, J = 6.4 Hz, 6H), 3.79 (s, 3H), 5.16 (m, 1H), 6.87 (d, J = 2.4 Hz, 1H), 6.96 (dd, J = 8.8 and 2.4 Hz, 1H), 7.36 (d, J = 9.2 Hz, 1H), 12.0 (s, 1H). MS (ESI): $[M]^+$ = 312.2, 314.2.

*5.1.4.6. Methyl 3-bromo-6-methoxy-1H-indole-2-carboxylate (**10f**).* Following general procedure C, petroleum ether was added to the residue, the mixture stirred for 15 min, and the resulting precipitate was collected by filtration to furnish the title compound **10f** as a brown solid (> 95% yield); mp 160–162 °C. ^{1}H NMR ($CDCl_3$) δ: 3.86 (s, 3H), 3.97 (s, 3H), 6.78 (d, J = 2.2 Hz, 1H), 6.86 (dd, J = 8.8 and 2.2 Hz, 1H), 7.34 (d, J = 8.8 Hz, 1H), 8.92 (bs, 1H). MS (ESI): $[M]^+$ = 284.1, 286.1.

*5.1.4.7. Methyl 3-bromo-7-methoxy-1H-indole-2-carboxylate (**10g**).* Following general procedure C, the crude residue purified by flash chromatography using ethyl acetate:petroleum ether 2:8 (v:v) as eluent furnished **10g** as a white solid. Yield: 81%, mp 176–178 °C. ^{1}H NMR ($CDCl_3$) δ: 3.97 (s, 3H), 3.98 (s, 3H), 6.75 (d, J = 5.0 Hz, 1H), 7.13 (t, J = 8.8 Hz, 1H), 7.23 (d, J = 5.0 Hz, 1H), 9.12 (bs, 1H). MS (ESI): $[M]^+$ = 284.1, 286.1.

*5.1.5. General method D for the synthesis of compounds **11a-p***

To a mixture of the appropriate 2-alkoxycarbonyl-3-bromo-1*H*-indole derivative **10a-g** (2 mmol) in DMF (10 mL) cooled at +4 °C (ice-water bath) was added sodium hydride (60% in mineral oil, 96 mg, 2.2 mmol, 1.1 equiv.) in small portions. After stirring for 30 min at room temperature, the appropriate alkyl halide (methyl, ethyl or propyl iodide) or benzyl bromide (4 mmol, 2 equiv.) was slowly added at +4 °C (ice-water bath), and the mixture was stirred for 4 h at room temperature. After this time, the reaction mixture was quenched by addition of a saturated aqueous solution of NH_4Cl (10 mL) and the product extracted with dichloromethane (3 × 10 mL). The combined organic extract was washed with water (10 mL) and brine, dried over Na_2SO_4 and concentrated under reduced pressure to furnish a residue that was purified by crystallization with the appropriate solvent or purified by flash chromatography on silica gel.

*5.1.5.1. Methyl 3-bromo-5-methyl-1-methyl-1H-indole-2-carboxylate (**11a**).* Following general procedure D, using iodomethane (284 mg, 0.12 mL) as alkylating agent, the crude residue was purified by flash chromatography, using EtOAc:petroleum ether 1:9 (v:v) as eluent, to furnish **11a** as a white solid. Yield: 77%, mp 120–121 °C. ^{1}H NMR (DMSO-d_6) δ: 2.42 (s, 3H), 3.90 (s, 3H), 3.97 (s, 3H), 7.20 (dd, J = 8.6 and 1.2 Hz, 1H), 7.34 (d, J = 1.2 Hz, 1H), 7.53 (d, J = 8.6 Hz, 1H). MS (ESI): $[M+1]^+$ = 282.1, 284.1.

*5.1.5.2. Methyl 3-bromo-5-methyl-1-benzyl-1H-indole-2-carboxylate (**11b**).* Following general procedure D, using benzyl bromide (342 mg, 0.25 mL) as alkylating agent, the crude residue was purified by flash chromatography, using EtOAc:petroleum ether 0.5:9.5 (v:v) as eluent, to furnish **11b** as a colorless oil. Yield: 81%. ^{1}H NMR (DMSO-d_6) δ: 2.42 (s, 3H), 3.84 (s, 3H), 5.80 (s, 2H), 6.97 (m, 2H), 7.23 (m, 4H), 7.38 (s, 1H), 7.55 (d, J = 8.8 Hz, 1H). MS (ESI): $[M+1]^+$ = 358.0, 360.2.

*5.1.5.3. Methyl 3-bromo-5-methoxy-1-methyl-1H-indole-2-carboxylate (**11c**).* Following general procedure D, using iodomethane (284 mg, 0.12 mL) as alkylating agent, the crude residue was purified by flash chromatography, using EtOAc:petroleum ether 1:9 (v:v) as eluent, to furnish **11c** as a white solid. Yield: 64%, mp 110–111 °C. ^{1}H NMR (DMSO-d_6) δ: 3.82 (s, 3H), 3.90 (s, 3H), 3.97 (s, 3H), 6.93 (d, J = 2.2 Hz, 1H), 7.02 (dd, J = 9.4 and 2.2 Hz, 1H), 7.57 (d, J = 9.4 Hz, 1H). MS (ESI): $[M+1]^+$ = 298.3, 300.3.

*5.1.5.4. Methyl 3-bromo-5-methoxy-1-ethyl-1H-indole-2-carboxylate (**11d**).* Following general procedure D, using iodoethane (312 mg, 0.16 mL) as alkylating agent, the crude residue was purified by flash chromatography, using EtOAc:petroleum ether 1:9 (v:v) as eluent, to furnish **11d** as an orange oil. Yield: > 95%. ^{1}H NMR ($CDCl_3$) δ: 1.37 (t, J = 7.2 Hz, 3H), 3.89 (s, 3H), 3.97 (s, 3H), 4.56 (q, J = 7.2 Hz, 2H), 7.03 (d, J = 2.2 Hz, 1H), 7.15 (d, J = 8.8 and 2.2 Hz, 1H), 7.36 (d, J = 8.8 Hz, 1H). MS (ESI): $[M+1]^+$ = 312.1, 314.2.

*5.1.5.5. Methyl 3-bromo-5-methoxy-1-n-propyl-1H-indole-2-carboxylate (**11e**).* Following general procedure D, using 1-iodopropane (0.34 g, 0.20 mL) as alkylating agent, the crude residue was purified by flash chromatography, using EtOAc:petroleum ether 1:9 (v:v) as eluent, to furnish **11e** as a colorless oil. Yield: 83%. ^{1}H NMR (DMSO-d_6) δ: 0.80 (t, J = 7.4 Hz, 3H), 1.65 (m, 2H), 3.82 (s, 3H), 3.90 (s, 3H), 4.47 (t, J = 7.2 Hz, 2H), 6.92 (d, J = 2.4 Hz, 1H), 7.03 (dd, J = 9.2 and 2.4 Hz, 1H), 7.61 (d, J = 9.2 Hz, 1H). MS (ESI): $[M+1]^+$ = 326.3, 328.3.

*5.1.5.6. Methyl 3-bromo-5-methoxy-1-benzyl-1H-indole-2-carboxylate (**11f**).* Following general procedure D, using benzyl bromide (342 mg, 0.25 mL) as alkylating agent, the crude residue was purified by flash chromatography, using EtOAc:petroleum ether 1:9 (v:v) as eluent, to furnish **11f** as a white solid. Yield: 73%, mp 112–114 °C. ^{1}H

NMR (DMSO-d_6) δ: 3.80 (s, 3H), 3.83 (s, 3H), 5.78 (s, 2H), 6.95 (m, 3H), 7.02 (d, J = 9.2 and 2.4 Hz, 1H), 7.19 (m, 3H), 7.58 (d, J = 9.2 Hz, 1H). MS (ESI): $[M+1]^+$ = 374.1, 376.3.

5.1.5.7. Ethyl 3-bromo-5-methoxy-1-methyl-1H-indole-2-carboxylate ***(11g)***. Following general procedure D, using iodomethane (284 mg, 0.12 mL) as alkylating agent, the crude residue was purified by flash chromatography, using EtOAc:petroleum ether 1:9 (v:v) as eluent, to furnish **11g** as a cream colored solid. Yield: 67%, mp 123–124 °C. ^{1}H NMR (DMSO-d_6) δ: 1.34 (t, J = 7.2 Hz, 3H), 3.82 (s, 3H), 3.97 (s, 3H), 4.32 (q, J = 7.0 Hz, 2H), 6.92 (d, J = 2.4 Hz, 1H), 7.04 (d, J = 9.0 and 2.4 Hz, 1H), 7.56 (d, J = 9.0 Hz, 1H). MS (ESI): $[M+1]^+$ = 312.2, 314.2.

5.1.5.8. Ethyl 3-bromo-5-methoxy-1-benzyl-1H-indole-2-carboxylate ***(11h)***. Following general procedure D, using benzyl bromide (342 mg, 0.25 mL) as alkylating agent, the crude residue was purified by flash chromatography, using EtOAc:petroleum ether 2:8 (v:v) as eluent, to furnish **11h** as a white solid. Yield: 71%, mp 124–126 °C. ^{1}H NMR (DMSO-d_6) δ: 1.34 (t, J = 7.2 Hz, 3H), 3.87 (s, 3H), 4.20 (q, J = 7.2 Hz, 2H), 5.78 (s, 2H), 6.88 (d, J = 1.2 Hz, 1H), 6.93 (m, 1H), 7.03 (dd, J = 9.2 and 1.2 Hz, 1H), 7.21 (m, 4H), 7.63 (d, J = 8.8 Hz, 1H). MS (ESI): $[M+1]^+$ = 388.1, 390.2.

5.1.5.9. n-Propyl 3-bromo-5-methoxy-1-methyl-1H-indole-2-carboxylate ***(11i)***. Following general procedure D, using iodomethane (284 mg, 0.12 mL) as alkylating agent, the crude residue was purified by flash chromatography, using EtOAc:petroleum ether 1:9 (v:v) as eluent, to furnish **11i** as a white solid. Yield: 58%, mp 141–143 °C. ^{1}H NMR (DMSO-d_6) δ: 1.03 (t, J = 7.2 Hz, 3H), 1.75 (m, 2H), 3.82 (s, 3H), 3.98 (s, 3H), 4.26 (t, J = 7.2 Hz, 2H), 6.92 (d, J = 2.4 Hz, 1H), 7.04 (dd, J = 9.0 and 2.4 Hz, 1H), 7.57 (d, J = 9.0 Hz, 1H). MS (ESI): $[M+1]^+$ = 326.2, 328.3.

5.1.5.10. n-Propyl 3-bromo-5-methoxy-1-benzyl-1H-indole-2-carboxylate ***(11j)***. Following general procedure D, using benzyl bromide (342 mg, 0.25 mL) as alkylating agent, the crude residue was purified by flash chromatography, using EtOAc:petroleum ether 0.5:9.5 (v:v) as eluent, to furnish **11j** as a colorless oil. Yield: 72%. ^{1}H NMR (DMSO-d_6) δ: 0.94 (t, J = 7.2 Hz, 3H), 1.67 (m, 2H), 3.83 (s, 3H), 4.23 (t, J = 6.4 Hz, 2H), 5.80 (s, 2H), 6.95 (m, 4H), 7.06 (dd, J = 9.0 and 2.2 Hz, 1H), 7.23 (m, 2H), 7.56 (d, J = 9.0 Hz, 1H). MS (ESI): $[M+1]^+$ = 403.1, 405.1.

5.1.5.11. Isopropyl 3-bromo-5-methoxy-1-methyl-1H-indole-2-carboxylate ***(11k)***. Following general procedure D, using iodomethane (284 mg, 0.12 mL) as alkylating agent, the crude residue was purified by flash chromatography, using EtOAc:petroleum ether 1:9 (v:v) as eluent, to furnish **11k** as a white solid. Yield: 75%, mp 102–104 °C. ^{1}H NMR (DMSO-d_6) δ: 1.36 (d, J = 6.4 Hz, 6H), 3.82 (s, 3H), 3.96 (s, 3H), 5.20 (m, 1H), 6.91 (d, J = 2.2 Hz, 1H), 7.03 (dd, J = 9.2 and 2.4 Hz, 1H), 7.56 (d, J = 9.2 Hz, 1H). MS (ESI): $[M+1]^+$ = 326.1, 328.2.

5.1.5.12. Isopropyl 3-bromo-5-methoxy-1-benzyl-1H-indole-2-carboxylate ***(11l)***. Following general procedure D, using benzyl bromide (342 mg, 0.25 mL) as alkylating agent, the crude residue was purified by flash chromatography, using EtOAc:petroleum ether 0.5:9.5 (v:v) as eluent, to furnish **11l** as a colorless, viscous oil. Yield: 81%. ^{1}H NMR (DMSO-d_6) δ: 1.25 (d, J = 6.2 Hz, 6H), 3.82 (s, 3H), 5.13 (m, 1H), 5.76 (s, 2H), 6.96 (m, 3H), 6.99 (dd, J = 9.0 and 2.4 Hz, 1H), 7.07 (m, 3H), 7.58 (d, J = 9.0 Hz, 1H). MS (ESI): $[M+1]^+$ = 402.1, 404.1.

5.1.5.13. Methyl 3-bromo-6-methoxy-1-methyl-1H-indole-2-carboxylate ***(11m)***. Following general procedure D, using iodomethane (284 mg, 0.12 mL) as alkylating agent, the crude residue was purified by flash chromatography, using EtOAc:petroleum ether 1:9 (v:v) as eluent, to furnish **11m** as a white solid. Yield: 82%, mp 108–110 °C. ^{1}H NMR ($CDCl_3$) δ: 3.89 (s, 3H), 3.96 (s, 3H), 3.99 (s, 3H), 6.72 (d, J = 2.2 Hz, 1H), 6.86 (dd, J = 8.8 and 2.2 Hz, 1H), 7.51 (d, J = 8.8 Hz, 1H). MS (ESI): $[M+1]^+$ = 298.3, 300.3.

5.1.5.14. Methyl 3-bromo-6-methoxy-1-ethyl-1H-indole-2-carboxylate ***(11n)***. Following general procedure D, using iodoethane (312 mg, 0.16 mL) as alkylating agent, the crude residue was purified by flash chromatography, using EtOAc:petroleum ether 1:9 (v:v) as eluent, to furnish **11n** as a white solid. Yield: 74%, mp 105–106 °C. ^{1}H NMR ($CDCl_3$) δ: 1.34 (t, J = 7.0 Hz, 3H), 3.89 (s, 3H), 3.96 (s, 3H), 4.51 (q, J = 7.0 Hz, 2H), 6.73 (d, J = 2.0 Hz, 1H), 6.86 (dd, J = 9.0 and 2.0 Hz, 2H), 7.52 (d, J = 9.0 Hz, 1H). MS (ESI): $[M+1]^+$ = 312.1, 314.2.

5.1.5.15. Methyl 3-bromo-6-methoxy-1-benzyl-1H-indole-2-carboxylate ***(11o)***. Following general procedure D, using benzyl bromide (342 mg, 0.25 mL) as alkylating agent, the crude residue was purified by flash chromatography, using EtOAc:petroleum ether 1:9 (v:v) as eluent, to furnish **11o** as a yellow oil. Yield: 68%. ^{1}H NMR ($CDCl_3$) δ: 3.80 (s, 3H), 3.88 (s, 3H), 5.75 (s, 2H), 6.69 (d, J = 2.2 Hz, 1H), 6.87 (d, J = 8.8 and 2.2 Hz, 1H), 7.02 (m, 2H), 7.24 (m, 3H), 7.55 (d, J = 8.8 Hz, 1H). MS (ESI): $[M+1]^+$ = 374.1, 376.1.

5.1.5.16. Methyl 3-bromo-7-methoxy-1-methyl-1H-indole-2-carboxylate ***(11p)***. Following general procedure D, using iodomethane (284 mg, 0.12 mL) as alkylating agent, the crude residue was purified by flash chromatography, using EtOAc:petroleum ether 1:9 (v:v) as eluent, to furnish **11p** as a white solid. Yield: 86%, mp 122–124 °C. ^{1}H NMR ($CDCl_3$) δ: 3.93 (s, 3H), 3.96 (s, 3H), 4.30 (s, 3H), 6.72 (d, J = 9.6 Hz, 1H), 7.06 (t, J = 9.6 Hz, 1H), 7.22 (d, J = 9.6 Hz, 1H). MS (ESI): $[M+1]^+$ = 298.2, 300.2.

5.1.6. General method E for the synthesis of compounds ***3a-ac***

To a dry Schlenk tube, 3-amino-2-alkoxycarbonyl-1*H*-indole derivative **8a-h** or *N*-1-substituted 2-alkoxycarbonyl-3-bromoindole **11a-p** (0.5 mmol) was dissolved in dry toluene (5 mL). $Pd(OAc)_2$ (6 mol%, 30 mg), *rac*-BINAP (4 mol%, 30 mg), Cs_2CO_3 (228 mg, 0.7 mmol, 1.4 equiv.) and 5-bromo-1,2,3-trimethoxybenzene (148 mg, 0.6 mmol, 1.2 equiv.) for the synthesis of compounds **3a-h**, 5-bromo-1,3-dimethoxybenzene (130 mg, 0.6 mmol, 1.2 equiv.) for the preparation of derivatives **3i-j**, 3,4,5-trimethoxyaniline (183 mg, 1 mmol, 2 equiv.) for the synthesis of compounds **3k-z** or 3,5-dimethoxyaniline (153 mg, 1 mmol, 2 equiv.) for the preparation of derivatives **3a-j** was added under argon, and the mixture was heated with stirring at 120 °C for 18 h. Upon cooling, dichloromethane was added (5 mL), the mixture was filtered through Celite under vacuum and the filtrate diluted with dichloromethane (10 mL) and water (5 mL). The aqueous phase was separated and additionally extracted with dichloromethane (2 × 5 mL). The combined organic phase was washed with brine (5 mL), dried over Na_2SO_4 and concentrated under reduced pressure to give a residue purified by flash column chromatography on silica gel.

5.1.6.1. Methyl 3-[(3,4,5-trimethoxyphenyl)amino]-1H-indole-2-carboxylate ***(3a)***. Following general procedure E, the crude residue obtained from **8a** and 5-bromo-1,2,3-trimethoxybenzene was purified by flash chromatography, using ethyl acetate:petroleum ether 3:7 (v:v) as eluent, to furnish **3a** as a green solid. Yield: 61%, mp 193 °C. ^{1}H NMR (DMSO-d_6) δ: 3.57 (s, 3H), 3.58 (s, 6H), 3.83 (s, 3H), 6.23 (s, 2H), 6.92 (t, J = 6.8 Hz, 1H), 7.22 (t, J = 6.8 Hz, 1H), 7.26 (d, J = 9.0 Hz, 1H), 7.33 (d, J = 9.0 Hz, 1H), 7.69 (s, 1H), 11.4 (s, 1H). ^{13}C NMR (DMSO-d_6) δ: 51.82, 55.89 (2C), 60.63, 94.34 (2C), 113.37, 114.75, 118.93, 120.78, 122.22, 125.93, 127.46, 131.20, 136.43, 141.25, 153.52 (2C), 162.57. MS (ESI): $[M+1]^+$ = 357.2. Anal. calcd for $C_{19}H_{20}N_2O_5$: C, 64.04; H, 5.66; N, 7.86; found: C, 63.89; H, 5.51; N, 7.64.

*5.1.6.2. Ethyl 3-[(3,4,5-trimethoxyphenyl)amino]-1H-indole-2-carboxylate (**3b**)*. Following general procedure E, the crude residue obtained from **8b** and 5-bromo-1,2,3-trimethoxybenzene was purified by flash chromatography, using ethyl acetate:petroleum ether 3:7 (v:v) as eluent, to furnish **3b** as a green solid. Yield: 45%, mp 121–122 °C. ^{1}H NMR ($CDCl_3$) δ: 1.30 (t, J = 7.2 Hz, 3H), 3.58 (s, 6H), 3.60 (s, 3H), 4.30 (q, J = 7.2 Hz, 2H), 6.24 (s, 2H), 6.72 (t, J = 8.4 Hz, 1H), 7.26 (m, 1H), 7.39 (m, 2H), 7.69 (s, 1H), 11.4 (s, 1H). ^{13}C NMR (DMSO-d_6) δ: 14.25, 55.37 (2C), 59.91, 60.09, 93.63 (2C), 112.84, 114.57, 118.46, 120.49, 121.54, 125.37, 126.84, 130.59, 135.80, 140.94, 153.02 (2C), 161.63. MS (ESI): $[M+1]^+$ = 371.21. Anal. calcd for $C_{20}H_{22}N_2O_5$: C, 64.85; H, 5.99; N, 7.56; found: C, 64.67; H, 5.78; N, 7.34.

*5.1.6.3. tert-Butyl 3-[(3,4,5-trimethoxyphenyl)amino]-1H-indole-2-carboxylate (**3c**)*. Following general procedure E, the crude residue obtained from **8c** and 5-bromo-1,2,3-trimethoxybenzene was purified by flash chromatography, using ethyl acetate:petroleum ether 2:8 (v:v) as eluent, to furnish **3c** as a yellow solid. Yield: 44%, mp 235 °C. ^{1}H NMR ($CDCl_3$) δ: 1.65 (s, 9H), 3.73 (s, 6H), 3.82 (s, 3H), 6.30 (s, 2H), 6.97 (m, 1H), 7.32 (m, 2H), 7.43 (d, J = 9.0 Hz, 1H), 7.48 (d, J = 9.0 Hz, 1H), 8.12 (bs, 1H). ^{13}C NMR ($CDCl_3$) δ: 28.63 (3C), 56.01 (2C), 61.18, 81.96, 95.83 (2C), 112.08, 113.79, 118.97, 120.36, 123.09, 126.23, 129.74, 132.57, 135.59, 140.00, 153.64 (2C), 162.14. MS (ESI): $[M+1]^+$ = 399.4. Anal. calcd for $C_{22}H_{26}N_2O_5$: C, 66.32; H, 6.58; N, 7.03; found: C, 66.12; H, 6.35; N, 6.89.

*5.1.6.4. Benzyl 3-[(3,4,5-trimethoxyphenyl)amino]-1H-indole-2-carboxylate (**3d**)*. Following general procedure E, the crude residue obtained from **8d** and 5-bromo-1,2,3-trimethoxybenzene was purified by flash chromatography, using ethyl acetate:petroleum ether 2:8 (v:v) as eluent, to furnish **3d** as a yellow solid. Yield: 52%, mp 171 °C. ^{1}H NMR ($CDCl_3$) δ: 3.72 (s, 6H), 3.82 (s, 3H), 5.38 (s, 2H), 6.23 (s, 2H), 7.02 (m, 1H), 7.29 (d, J = 3.4 Hz, 1H), 7.41 (m, 8H), 8.12 (s, 1H). ^{13}C NMR ($CDCl_3$) δ: 56.01 (2C), 61.18, 66.41, 96.25 (2C), 112.08, 112.20, 119.09, 120.05, 123.21, 126.72, 128.53 (2C), 128.62, 128.82 (2C), 131.10, 132.85, 135.89, 136.22, 139.58, 153.64 (2C), 162.28. MS (ESI): $[M+1]^+$ = 433.47. Anal. calcd for $C_{25}H_{24}N_2O_5$: C, 69.43; H, 5.59; N, 6.48; found: C, 69.16; H, 5.37; N, 6.24.

*5.1.6.5. Ethyl 6-chloro-3-[(3,4,5-trimethoxyphenyl)amino]-1H-indole-2-carboxylate (**3e**)*. Following general procedure E, the crude residue obtained from **8e** and 5-bromo-1,2,3-trimethoxybenzene was purified by flash chromatography, using ethyl acetate:petroleum ether 3:7 (v:v) as eluent, to furnish **3e** as a yellow solid. Yield: 52%, mp 195 °C. ^{1}H NMR ($CDCl_3$) δ: 1.42 (t, J = 7.2 Hz, 3H), 3.74 (s, 6H), 3.82 (s, 3H), 4.39 (q, J = 7.0 Hz, 2H), 6.29 (s, 2H), 6.92 (dd, J = 7.8 and 1.6 Hz, 1H), 7.32 (dd, J = 7.8 and 1.6 Hz, 1H),), 7.40 (m, 2H), 8.20 (bs, 1H). ^{13}C NMR ($CDCl_3$) δ: 30.92, 55.98 (2C), 60.68, 61.08, 96.61 (2C), 111.79, 112.62, 118.02, 119.89, 124.04, 132.46, 136.81, 138.13, 139.14, 152.12, 153.60 (2C), 162.20. MS (ESI): $[M+1]^+$ = 405.4. Anal. calcd for $C_{20}H_{21}ClN_2O_5$: C, 59.33; H, 5.23; N, 6.92; found: C, 59.05; H, 5.02; N, 6.77.

*5.1.6.6. Methyl 5-methoxy-3-[(3,4,5-trimethoxyphenyl)amino]-1H-indole-2-carboxylate (**3f**)*. Following general procedure E, the crude residue obtained from **8f** and 5-bromo-1,2,3-trimethoxybenzene was purified by flash chromatography, using ethyl acetate:petroleum ether 4:6 (v:v) as eluent, to furnish **3f** as a yellow solid. Yield: 53%, mp 107 °C. ^{1}H NMR ($CDCl_3$) δ: 3.57 (s, 3H), 3.61 (s, 6H), 3.63 (s, 3H), 3.83 (s, 3H), 6.19 (s, 2H), 6.69 (d, J = 2.4 Hz, 1H), 6.93 (dd, J = 9.2 and 2.4 Hz, 1H), 7.29 (d, J = 9.2 Hz, 1H), 7.63 (s, 1H), 11.3 (s, 1H). ^{13}C NMR ($CDCl_3$) δ: 51.25, 55.09, 55.40 (2C), 60.10, 93.29 (2C), 101.24, 113.94, 115.45, 117.16, 120.70, 126.06, 130.35, 131.27, 141.09, 152.41, 153.03 (2C), 161.86. MS (ESI): $[M+1]^+$ = 387.4. Anal. calcd for $C_{20}H_{22}N_2O_6$: C, 62.17; H, 5.74; N, 7.25; found: C, 62.01; H, 5.37; N, 7.01.

*5.1.6.7. Ethyl 5-methoxy-3-[(3,4,5-trimethoxyphenyl)amino]-1H-indole-2-carboxylate (**3g**)*. Following general procedure E, the crude residue obtained from **8g** and 5-bromo-1,2,3-trimethoxybenzene was purified by flash chromatography, using ethyl acetate:petroleum ether 3:7 (v:v) as eluent, to furnish **3g** as a yellow solid. Yield: 43%, mp 165–166 °C. ^{1}H NMR (DMSO-d_6) δ: 1.27 (t, J = 7.2 Hz, 3H), 3.57 (s, 3H), 3.61 (s, 6H), 3.64 (s, 3H), 4.27 (q, J = 7.2 Hz, 2H), 6.17 (s, 2H), 6.74 (d, J = 2.8 Hz, 1H), 6.93 (dd, J = 9.2 and 2.8 Hz, 1H), 7.31 (d, J = 8.8 Hz, 1H), 7.60 (s, 1H), 11.3 (s, 1H). ^{13}C NMR ($CDCl_3$) δ: 14.19, 55.09, 55.39 (2C), 59.83, 60.07, 93.06 (2C), 101.03, 113.91 (2C), 115.87, 117.10, 121.02, 125.91, 131.14, 141.38, 152.51, 153.03 (2C), 161.43. MS (ESI): $[M+1]^+$ = 401.34. Anal. calcd for $C_{21}H_{24}N_2O_6$: C, 62.99; H, 6.04; N, 7.00; found: C, 62.73; H, 5.89; N, 6.87.

*5.1.6.8. Methyl 6-methoxy-3-[(3,4,5-trimethoxyphenyl)amino]-1H-indole-2-carboxylate (**3h**)*. Following general procedure E, the crude residue obtained from **8h** and 5-bromo-1,2,3-trimethoxybenzene was purified by flash chromatography, using ethyl acetate:petroleum ether 3:7 (v:v) as eluent, to furnish **3h** as a yellow solid. Yield: 52%, mp 144–146 °C. ^{1}H NMR ($CDCl_3$) δ: 3.74 (s, 3H), 3.85 (s, 6H), 3.89 (s, 3H), 4.00 (s, 3H), 6.44 (s, 2H), 6.62 (d, J = 9.2 Hz, 1H), 6.91 (dd, J = 9.2 and 2.4 Hz, 1H), 7.02 (d, J = 2.4 Hz, 1H), 8.10 (s, 1H), 11.3 (bs, 1H). ^{13}C NMR ($CDCl_3$) δ: 51.21, 55.13, 55.40 (2C), 60.02, 93.33 (2C), 101.55, 113.78, 115.40, 117.54, 121.12, 126.33, 130.29, 131.31, 141.00, 152.40, 153.12 (2C), 161.55. MS (ESI): $[M+1]^+$ = 387.3. Anal. calcd for $C_{20}H_{22}N_2O_6$: C, 62.17; H, 5.74; N, 7.25; found: C, 61.92; H, 5.52; N, 7.03.

*5.1.6.9. Methyl 3-[(3,5-dimethoxyphenyl)amino]-1H-indole-2-carboxylate (**3i**)*. Following general procedure E, the crude residue obtained from **8a** and 5-bromo-1,3-dimethoxybenzene was purified by flash chromatography, using ethyl acetate:petroleum ether 2:8 (v:v) as eluent, to furnish **3i** as an orange solid. Yield: 80%, mp 138–140 °C. ^{1}H NMR ($CDCl_3$) δ: 3.71 (s, 6H), 3.94 (s, 3H), 6.10 (bs, 1H), 6.22 (s, 2H), 6.99 (m, 1H), 7.32 (m, 3H), 7.52 (d, J = 8.4 Hz, 1H), 8.25 (bs, 1H). ^{13}C NMR (DMSO-d_6) δ: 51.30, 54.71 (2C), 91.02, 93.89, 111.98, 112.79, 115.60, 117.59, 118.70, 120.39, 121.18, 125.24, 125.76, 135.65, 146.99, 160.76, 161.78. MS (ESI): $[M+1]^+$ = 327.3. Anal. calcd for $C_{18}H_{18}N_2O_4$: C, 66.25; H, 5.56; N, 8.58; found: C, 66.02; H, 5.35; N, 8.35.

*5.1.6.10. Ethyl 3-[(3,5-dimethoxyphenyl)amino]-1H-indole-2-carboxylate (**3j**)*. Following general procedure E, the crude residue obtained from **8b** and 5-bromo-1,3-dimethoxybenzene was purified by flash chromatography, using ethyl acetate:petroleum ether 2:8 (v:v) as eluent, to furnish **3j** as a yellow solid. Yield: 52%, mp 142 °C. ^{1}H NMR ($CDCl_3$) δ: 1.41 (t, J = 7.0 Hz, 3H), 3.71 (s, 6H), 4.42 (q, J = 7.0 Hz, 2H), 6.10 (s, 1H), 6.22 (s, 2H), 6.99 (t, J = 8.4 Hz, 1H), 7.33 (m, 3H), 7.53 (t, J = 8.4 Hz, 1H), 8.22 (bs, 1H). ^{13}C NMR ($CDCl_3$) δ: 14.15, 54.70 (2C), 59.92, 90.93, 93.71 (2C), 112.78, 115.94, 118.75, 120.25, 121.20, 121.40, 125.21, 125.67, 135.55, 147.18 (2C), 160.78. MS (ESI): $[M+1]^+$ = 341.4. Anal. calcd for $C_{19}H_{20}N_2O_4$: C, 67.05; H, 5.92; N, 8.23; found: C, 66.89; H, 5.73; N, 8.03.

*5.1.6.11. Methyl 1,5-dimethyl-3-[(3,4,5-trimethoxyphenyl)amino]-1H-indole-2-carboxylate (**3k**)*. Following general procedure E, the crude residue obtained from **11a** and 3,4,5-trimethoxyaniline was purified by flash chromatography, using ethyl acetate:petroleum ether 3:7 (v:v) as eluent, to furnish **3k** as a yellow solid. Yield: 42%, mp 134–136 °C. ^{1}H NMR (DMSO-d_6) δ: 2.31 (s, 3H), 3.58 (s, 3H), 3.59 (s, 6H), 3.83 (s, 3H), 3.90 (s, 3H), 6.21 (s, 2H), 7.16 (d, J = 1.2 Hz, 1H), 7.22 (dd, J = 9.2 and 1.2 Hz, 1H), 7.45 (d, J = 9.2 Hz, 1H), 7.74 (s, 1H). ^{13}C NMR (DMSO-d_6) δ: 20.86, 31.91, 51.36, 55.39 (2C), 60.10, 93.68 (2C), 110.77, 116.41, 119.80, 120.82, 127.15, 127.50, 127.66, 130.66, 136.44, 140.98, 153.01 (2C), 162.29. MS (ESI): $[M+1]^+$ = 384.9. Anal. calcd for $C_{21}H_{24}N_2O_5$: C, 65.61; H, 6.29; N, 7.29; found: C, 65.36; H, 6.07; N, 7.13.

*5.1.6.12. Methyl 5-methyl-1-benzyl-3-[(3,4,5-trimethoxyphenyl)amino]-1H-indole-2-carboxylate (**3l**)*. Following general procedure E, the crude residue obtained from **11b** and 3,4,5-trimethoxyaniline was purified by flash chromatography, using ethyl acetate:petroleum ether 3:7 (v:v) as eluent, to furnish **3l** as a yellow solid. Yield: 49%, mp 138–139 °C. ^{1}H NMR (DMSO-d_6) δ: 2.30 (s 3H), 3.59 (s, 3H), 3.60 (s, 6H), 3.75 (s, 3H), 5.73 (s, 2H), 6.22 (s, 2H), 6.96 (dd, J = 8.8 and 1.2 Hz, 1H), 7.18 (m, 3H), 7.23 (m, 3H), 7.49 (d, J = 8.8 Hz, 1H), 7.81 (s, 1H). ^{13}C NMR (DMSO-d_6) δ: 20.85, 47.26, 51.32, 55.41 (2C), 60.12, 88.66, 93.90 (2C), 111.22, 115.82, 120.28, 120.96, 126.05 (2C), 126.89, 128.01, 128.20, 128.35 (2C), 120.75, 136.55, 138.77, 140.89, 153.01 (2C), 162.10. MS (ESI): $[M+1]^+$ = 461.4. Anal. calcd for $C_{27}H_{28}N_2O_5$: C, 70.42; H, 6.13; N, 6.08; found: C, 70.21; H, 6.01; N, 5.88.

*5.1.6.13. Methyl 5-methoxy-1-methyl-3-[(3,4,5-trimethoxyphenyl)amino]-1H-indole-2-carboxylate (**3m**)*. Following general procedure E, the crude residue obtained from **11c** and 3,4,5-trimethoxyaniline was purified by flash chromatography, using ethyl acetate:petroleum ether 3:7 (v:v) as eluent, to furnish **3m** as a yellow solid. Yield: 51%, mp 114–115 °C. ^{1}H NMR (DMSO-d_6) δ: 3.57 (s, 3H), 3.61 (s, 6H), 3.63 (s, 3H), 3.82 (s, 3H), 3.91 (s, 3H), 6.18 (s, 2H), 6.70 (d, J = 2.4 Hz, 1H), 7.00 (d, J = 9.2 and 2.4 Hz, 1H), 7.49 (d, J = 9.2 Hz, 1H), 7.69 (s, 1H). ^{13}C NMR ($CDCl_3$) δ: 31.97, 51.34, 55.14, 55.40 (2C), 60.07, 93.49 (2C), 101.43, 109.34, 112.18, 117.18, 118.73, 119.88, 126.88, 133.33, 141.10, 152.60, 153.01 (2C), 161.16. MS (ESI): $[M+1]^+$ = 401.4. Anal. calcd for $C_{21}H_{24}N_2O_6$: C, 62.99; H, 6.04; N, 7.00; found: C, 62.77; H, 5.89; N, 6.78.

*5.1.6.14. Methyl 5-methoxy-1-ethyl-3-[(3,4,5-trimethoxyphenyl)amino]-1H-indole-2-carboxylate (**3n**)*. Following general procedure E, the crude residue obtained from **11d** and 3,4,5-trimethoxyaniline was purified by flash chromatography using ethyl acetate:petroleum ether 3:7 (v:v) as eluent, to furnish **3n** as a yellow solid. Yield: 48%, mp 150–151 °C. ^{1}H NMR (DMSO-d_6) δ: 1.21 (t, J = 7.2 Hz, 3H), 3.57 (s, 3H), 3.61 (s, 6H), 3.63 (s, 3H), 3.81 (s, 3H), 4.47 (q, J = 7.2 Hz, 2H), 6.17 (s, 2H), 6.71 (d, J = 2.4 Hz, 1H), 7.00 (d, J = 2.4 and 9.2 Hz, 1H), 7.51 (d, J = 9.2 Hz, 1H), 7.70 (s, 1H). ^{13}C NMR (DMSO-d_6) δ: 13.99, 15.49, 51.36, 55.16, 55.42 (2C), 60.09, 93.56 (2C), 101.62, 112.05, 116.01, 117.24, 120.12, 127.22, 130.49, 132.41, 141.10, 152.65, 153.02 (2C), 161.98. MS (ESI): $[M+1]^+$ = 414.8. Anal. calcd for $C_{22}H_{26}N_2O_6$: C, 63.76; H, 6.32; N, 6.76; found: C, 63.57; H, 6.11; N, 6.47.

*5.1.6.15. Methyl 5-methoxy-1-n-propyl-3-[(3,4,5-trimethoxyphenyl) amino]-1H-indole-2-carboxylate (**3o**)*. Following general procedure E, the crude residue obtained from **11e** and 3,4,5-trimethoxyaniline was purified by flash chromatography, using ethyl acetate:petroleum ether 3:7 (v:v) as eluent, to furnish **3o** as a yellow solid. Yield: 48%, mp 130–132 °C. ^{1}H NMR (DMSO-d_6) δ: 0.79 (t, J = 7.6 Hz, 3H), 1.63 (m, 2H), 3.57 (s, 3H), 3.60 (s, 6H), 3.63 (s, 3H), 3.80 (s, 3H), 4.41 (t, J = 7.2 Hz, 2H), 6.16 (s, 2H), 6.71 (d, J = 2.8 Hz, 1H), 7.01 (dd, J = 9.2 and 2.8 Hz, 1H), 7.52 (d, J = 9.2 Hz, 1H), 7.69 (s, 1H). ^{13}C NMR (DMSO-d_6) δ: 11.49, 24.02, 46.17, 51.88, 55.68, 55.93 (2C), 60.62, 93.95 (2C), 101.95, 112.89, 117.06, 117.71, 120.59, 127.60, 130.95, 133.48, 141.78, 153.17, 153.55 (2C), 162.59. MS (ESI): $[M+1]^+$ = 429.5. Anal. calcd for $C_{23}H_{28}N_2O_6$: C, 64.47; H, 6.59; N, 6.54; found: C, 64.21; H, 6.33; N, 6.36.

*5.1.6.16. Methyl 5-methoxy-1-benzyl-3-[(3,4,5-trimethoxyphenyl)amino]-1H-indole-2-carboxylate (**3p**)*. Following general procedure E, the crude residue obtained from **11f** and 3,4,5-trimethoxyaniline was purified by flash chromatography, using ethyl acetate:petroleum ether 3:7 (v:v) as eluent, to furnish **3p** as a brown solid. Yield: 48%, mp 138–139 °C. ^{1}H NMR (DMSO-d_6) δ: 3.58 (s, 3H), 3.61 (s, 6H), 3.64 (s, 3H), 3.73 (s, 3H), 5.74 (s, 2H), 6.19 (s, 2H), 6.83 (d, J = 2.4 Hz, 1H), 6.99 (m, 3H), 7.22 (m, 3H), 7.63 (d, J = 9.2 Hz, 1H), 7.77 (s, 1H). ^{13}C NMR ($CDCl_3$) δ: 47.32, 51.30, 55.14, 55.42 (2C), 60.09, 93.71 (2C), 101.62, 112.61, 116.56, 117.46, 120.47, 126.04 (2C), 126.91, 127.94, 128.36 (2C), 130.61, 133.37, 138.77, 141.06, 152.89, 153.02 (2C), 161.98. MS (ESI): $[M+1]^+$ = 477.5. Anal. calcd for $C_{27}H_{28}N_2O_6$: C, 68.05; H, 5.92; N, 5.88; found: C, 67.88; H, 5.71; N, 5.63.

*5.1.6.17. Ethyl 5-methoxy-1-methyl-3-[(3,4,5-trimethoxyphenyl)amino]-1H-indole-2-carboxylate (**3q**)*. Following general procedure E, the crude residue obtained from **11g** and 3,4,5-trimethoxyaniline was purified by flash chromatography, using ethyl acetate:petroleum ether 3:7 (v:v) as eluent, to furnish **3q** as a yellow solid. Yield: 46%, mp 94–95 °C. ^{1}H NMR (DMSO-d_6) δ: 1.22 (t, J = 7.2 Hz, 3H), 3.55 (s, 3H), 3.58 (s, 6H), 3.64 (s, 3H), 3.90 (s, 3H), 4.22 (q, J = 7.2 Hz, 2H), 6.13 (s, 2H), 6.75 (d, J = 2.4 Hz, 1H), 6.99 (dd, J = 9.2 and 2.4 Hz, 1H), 7.47 (d, J = 9.2 Hz, 1H), 7.63 (s, 1H). ^{13}C NMR ($CDCl_3$) δ: 13.92, 31.99, 55.16, 55.37 (2C), 60.06, 92.98 (2C), 101.09, 112.16, 117.15, 117.65, 120.33, 126.59, 130.26, 133.17, 141.53, 152.75, 153.05 (2C), 161.71. MS (ESI): $[M+1]^+$ = 415.0. Anal. calcd for $C_{22}H_{26}N_2O_6$: C, 63.76; H, 6.32; N, 6.76; found: C, 63.55; H, 6.122; N, 6.48.

*5.1.6.18. Ethyl 5-methoxy-1-benzyl-3-[(3,4,5-trimethoxyphenyl)amino]-1H-indole-2-carboxylate (**3r**)*. Following general procedure E, the crude residue obtained from **11h** and 3,4,5-trimethoxyaniline was purified by flash chromatography, using ethyl acetate:petroleum ether 3:7 (v:v) as eluent, to furnish **3r** as a yellow solid. Yield: 46%, mp 129–130 °C. ^{1}H NMR (DMSO-d_6) δ: 1.10 (t, J = 6.8 Hz, 3H), 3.57 (s, 3H), 3.61 (s, 6H), 3.67 (s, 3H), 4.15 (q, J = 7.2 Hz, 2H), 5.74 (s, 2H), 6.16 (s, 2H), 6.84 (d, J = 2.8 Hz, 1H), 6.94 (d, J = 6.8 Hz, 2H), 6.98 (dd, J = 9.2 and 2.8 Hz, 1H), 7.23 (m, 3H), 7.54 (d, J = 9.2 Hz, 1H), 7.74 (s, 1H). ^{13}C NMR (DMSO-d_6) δ: 13.72, 47.34, 55.15, 55.36 (2C), 60.04, 93.12 (2C), 99.16, 101.26, 112.54, 117.15, 117.43, 118.42, 120.92, 125.92 (2C), 126.86, 127.64, 128.31 (2C), 130.16, 133.20, 138.80, 141.51, 153.03 (2C), 161.54. MS (ESI): $[M+1]^+$ = 491.3. Anal. calcd for $C_{28}H_{30}N_2O_6$: C, 68.56; H, 6.16; N, 5.71; found: C, 68.32; H, 6.02; N, 5.52.

*5.1.6.19. n-Propyl 5-methoxy-1-methyl-3-[(3,4,5-trimethoxyphenyl) amino]-1H-indole-2-carboxylate (**3s**)*. Following general procedure E, the crude residue obtained from **11i** and 3,4,5-trimethoxyaniline was purified by flash chromatography, using ethyl acetate:petroleum ether 2:8 (v:v) as eluent, to furnish **3s** as a yellow solid. Yield: 43%, mp 112–113 °C. ^{1}H NMR (DMSO-d_6) δ: 0.89 (t, J = 7.2 Hz, 3H), 1.64 (m, 2H), 3.56 (s, 3H), 3.60 (s, 6H), 3.65 (s, 3H), 3.92 (s, 3H), 4.16 (t, J = 7.2 Hz, 2H), 6.14 (s, 2H), 6.76 (d, J = 2.4 Hz, 1H), 7.01 (dd, J = 8.8 and 2.4 Hz, 1H), 7.49 (d, J = 8.8 Hz, 1H), 7.63 (s, 1H). ^{13}C NMR (DMSO-d_6) δ: 10.40, 21.38, 32.05, 55.17, 55.39 (2C), 60.08, 65.65, 92.98 (2C), 101.12, 112.21, 117.19, 120.33, 126.64, 133.21, 141.49, 142.53, 149.95, 152.78, 153.06 (2C), 161.84. MS (ESI): $[M+1]^+$ = 429.5. Anal. calcd for $C_{23}H_{28}N_2O_6$: C, 64.47; H, 6.59; N, 6.54; found: C, 64.27; H, 6.37; N, 6.29.

*5.1.6.20. n-Propyl 5-methoxy-1-benzyl-3-[(3,4,5-trimethoxyphenyl) amino]-1H-indole-2-carboxylate (**3t**)*. Following general procedure E, the crude residue obtained from **11j** and 3,4,5-trimethoxyaniline was purified by flash chromatography, using ethyl acetate:petroleum ether 2:8 (v:v) as eluent, to furnish **3t** as a yellow solid. Yield: 56%, mp 107–109 °C. ^{1}H NMR (DMSO-d_6) δ: 0.74 (t, J = 7.6 Hz, 3H), 1.52 (m, 2H), 3.57 (s, 3H), 3.60 (s, 6H), 3.66 (s, 3H), 4.08 (t, J = 6.4 Hz, 2H), 5.75 (s, 2H), 6.15 (s, 2H), 6.83 (d, J = 2.2 Hz, 1H), 6.97 (m, 2H), 7.02 (dd, J = 9.0 and 2.2 Hz, 1H), 7.23 (m, 3H), 7.53 (d, J = 9.0 Hz, 1H), 7.73 (s, 1H). ^{13}C NMR (DMSO-d_6) δ: 10.77, 21.83, 47.90, 55.71, 55.91 (2C), 60.61, 66.18, 93.63 (2C), 101.81, 113.11, 117.85, 118.00 (2C), 121.49, 126.41 (2C), 127.41, 128.13, 128.88 (2C), 130.91, 133.75, 139.32, 142.03, 153.58 (2C), 162.21. MS (ESI): $[M+1]^+$ = 505.3. Anal. calcd for $C_{29}H_{32}N_2O_6$: C, 69.03; H, 6.39; N, 5.55; found: C, 58.78; H, 6.21; N, 5.32.

*5.1.6.21. Isopropyl 5-methoxy-1-methyl-3-[(3,4,5-trimethoxyphenyl) amino]-1H-indole-2-carboxylate (**3u**)*. Following general procedure E, the crude residue obtained from **11k** and 3,4,5-trimethoxyaniline was purified by flash chromatography, using ethyl acetate:petroleum ether 2:8 (v:v) as eluent, to furnish **3u** as a yellow solid. Yield: 52%, mp 157–159 °C. ^{1}H NMR (DMSO-d_6) δ: 1.22 (d, J = 6.0 Hz, 6H), 3.54 (s, 3H), 3.58 (s, 6H), 3.65 (s, 3H), 3.89 (s, 3H), 5.07 (m, 1H), 6.11 (s, 2H), 6.77 (d, J = 2.4 Hz, 1H), 6.99 (dd, J = 9.2 and 2.4 Hz, 1H), 7.47 (d, J = 9.2 Hz, 1H), 7.58 (s, 1H). ^{13}C NMR (DMSO-d_6) δ: 21.53 (2C), 32.08, 55.19, 55.40 (2C), 60.09, 67.75, 92.82 (2C), 100.96, 112.19, 117.15, 118.12, 120.55, 122.14, 126.45, 130.23, 133.11, 141.78, 152.85, 153.10, 161.28. MS (ESI): $[M+1]^+$ = 429.4. Anal. calcd for $C_{23}H_{28}N_2O_6$: C, 64.47; H, 6.59; N, 6.54; found: C, 64.26; H, 6.34; N, 6.21.

*5.1.6.22. Isopropyl 5-methoxy-1-benzyl-3-[(3,4,5-trimethoxyphenyl) amino]-1H-indole-2-carboxylate (**3v**)*. Following general procedure E, the crude residue obtained from **11l** and 3,4,5-trimethoxyaniline was purified by flash chromatography, using ethyl acetate:petroleum ether 3:7 (v:v) as eluent, to furnish **3v** as a yellow solid. Yield: 42%, mp 115–116 °C. ^{1}H NMR (DMSO-d_6) δ: 1.05 (d, J = 6.0 Hz, 6H), 3.54 (s, 3H), 3.58 (s, 6H), 3.66 (s, 3H), 4.96 (m, 1H), 5.72 (s, 2H), 6.12 (s, 2H), 6.85 (d, J = 2.4 Hz, 1H), 6.92 (d, J = 6.8 Hz, 2H), 6.94 (dd, J = 9.2 and 2.4 Hz, 1H), 7.22 (m, 3H), 7.53 (d, J = 9.2 Hz, 1H), 7.71 (s, 1H). ^{13}C NMR (DMSO-d_6) δ: 21.26 (2C), 47.43, 55.18, 55.36 (2C), 60.09, 67.66, 92.93 (2C), 101.10, 112.51, 117.41, 117.66, 121.12, 125.85 (2C), 126.86, 127.47, 128.31 (2C), 130.29, 133.12, 138.89, 141.78. 153.07, 153.14 (2C), 161.12. MS (ESI): $[M+1]^+$ = 505.5. Anal. calcd for $C_{29}H_{32}N_2O_6$: C, 69.03; H, 6.39; N, 5.55; found: C, 68,89; H, 6.26; N, 5.37.

*5.1.6.23. Methyl 6-methoxy-1-methyl-3-[(3,4,5-trimethoxyphenyl)amino]-1H-indole-2-carboxylate (**3w**)*. Following general procedure E, the crude residue obtained from **11m** and 3,4,5-trimethoxyaniline was purified by flash chromatography, using ethyl acetate:petroleum ether 2:8 (v:v) as eluent, to furnish **3w** as a white solid. Yield: 43%, mp 139–140 °C. ^{1}H NMR (DMSO-d_6) δ: 3.58 (s, 3H), 3.60 (s, 6H), 3.82 (s, 3H), 3.84 (s, 3H), 3.89 (s, 3H), 6.26 (s, 2H), 6.62 (dd, J = 8.8 and 2.4 Hz, 1H), 6.99 (d, J = 2.2 Hz, 1H), 7.18 (d, J = 8.8 Hz, 1H), 7.79 (s, 1H). ^{13}C NMR (DMSO-d_6) δ: 51.74, 55.44, 55.87, 55.99 (2C), 60.68, 93.12, 95.12 (2C), 110.87, 113.85, 114.82, 123.42, 129.75, 131.62, 139.98, 140.94, 153.59 (2C), 159.45, 162.82. MS (ESI): $[M+1]^+$ = 401.3. Anal. calcd for $C_{21}H_{24}N_2O_6$: C, 62.99; H, 6.04; N, 7.00; found: C, 62.78; H, 5.88; N, 6.78.

*5.1.6.24. Methyl 6-methoxy-1-ethyl-3-[(3,4,5-trimethoxyphenyl)amino]-1H-indole-2-carboxylate (**3x**)*. Following general procedure E, the crude residue obtained from **11n** and 3,4,5-trimethoxyaniline was purified by flash chromatography, using ethyl acetate:petroleum ether 3:7 (v:v) as eluent, to furnish **3x** as a yellow oil. Yield: 52%. ^{1}H NMR (DMSO-d_6) δ: 1.24 (t, J = 6.8 Hz, 3H), 3.59 (s, 3H), 3.61 (s, 6H), 3.82 (s, 3H), 3.84 (s, 3H), 4.46 (q, J = 6.8 Hz, 2H), 6.26 (s, 2H), 6.63 (dd, J = 8.8 and 1.6 Hz, 1H), 6.99 (d, J = 1.6 Hz, 1H), 7.19 (d, J = 8.8 Hz, 1H), 7.80 (s, 1H). ^{13}C NMR (DMSO-d_6) δ: 15.18, 51.14, 55.41 (2C), 59.66, 60.08, 80.38, 92.35, 94.61 (2C), 110.24, 113.03, 113.41, 122.97, 129.44, 131.03, 138.46, 140.27, 152.98 (2C), 158.87, 161.99. MS (ESI): $[M+1]^+$ = 415.3. Anal. calcd for $C_{22}H_{26}N_2O_6$: C, 63.76; H, 6.32; N, 6.76; found: C, 63.58; H, 6.11; N, 6.52.

*5.1.6.25. Methyl 5-methoxy-1-benzyl-3-[(3,4,5-trimethoxyphenyl)amino]-1H-indole-2-carboxylate (**3y**)*. Following general procedure E, the crude residue obtained from **11o** and 3,4,5-trimethoxyaniline was purified by flash chromatography, using ethyl acetate:petroleum ether 2:8 (v:v) as eluent, to furnish **3y** as a yellow oil. Yield: 56%. ^{1}H NMR (DMSO-d_6) δ: 3.59 (s, 3H), 3.61 (s, 6H), 3.73 (s, 3H), 3.77 (s, 3H), 5.27 (s, 2H), 6.28 (s, 2H), 6.83 (dd, J = 7.2 and 2.0 Hz, 1H), 7.00 (d, J = 7.2 Hz, 1H), 7.08 (d, J = 2.0 Hz, 1H), 7.24 (m, 5H), 7.86 (s, 1H). ^{13}C NMR ($CDCl_3$) δ: 51.07, 54.85, 55.32, 55.43, 60.10, 64.85, 93.13, 94.86 (2C), 110.39, 113.50, 113.63, 122.99, 126.21 (2C), 126.87, 128.36 (2C), 130.18, 131.19, 138.78, 139.63, 140.18, 152.99 (2C), 159.05, 161.99. MS (ESI): $[M+1]^+$ = 477.5. Anal. calcd for $C_{27}H_{28}N_2O_6$: C, 68.05; H, 5.92; N, 5.88; found: C, 67.89; H, 5.73; N, 5.65.

*5.1.6.26. Methyl 6-methoxy-1-methyl-3-[(3,4,5-trimethoxyphenyl)amino]-1H-indole-2-carboxylate (**3z**)*. Following general procedure E, the crude residue obtained from **11p** and 3,4,5-trimethoxyaniline was purified by flash chromatography, using ethyl acetate:petroleum ether 3:7 (v:v) as eluent, to furnish **3z** as a yellow solid. Yield: 54%, mp 156–158 °C. ^{1}H NMR (DMSO-d_6) δ: 3.55 (s, 3H), 3.56 (s, 6H), 3.79 (s, 3H), 3.89 (s, 3H), 4.14 (s, 3H), 4.14 (s, 2H), 6.82 (d, J = 9.2 Hz, 1H), 6.88 (m, 2H), 7.67 (bs, 1H). ^{13}C NMR (DMSO-d_6) δ: 35.30, 51.97, 55.88 (2C), 56.11, 60.61, 94.20 (2C), 106.75, 114.64, 118.02, 119.94, 122.78, 128.34, 129.13, 131.07, 141.61, 148.12, 153.50 (2C), 162.59. MS (ESI): $[M+1]^+$ = 401.3. Anal. calcd for $C_{21}H_{24}N_2O_6$: C, 62.99; H, 6.04; N, 7.00; found: C, 62.77; H, 5.78; N, 6.78.

*5.1.6.27. Methyl 5-methoxy-1-methyl-3-[(3,5-dimethoxyphenyl)amino]-1H-indole-2-carboxylate (**3aa**)*. Following general procedure E, the crude residue obtained from **11c** and 3,5-dimethoxyaniline was purified by flash chromatography, using ethyl acetate:petroleum ether 2:8 (v:v) as eluent, to furnish **3aa** as a yellow solid. Yield: 49%, mp 89–90 °C. ^{1}H NMR (DMSO-d_6) δ: 3.61 (s, 6H), 3.65 (s, 3H), 3.79 (s, 3H), 3.92 (s, 3H), 5.91 (d, J = 2.4 Hz, 1H), 5.97 (d, J = 2.4 Hz, 2H), 6.72 (d, J = 2.4 Hz, 1H), 7.01 (dd, J = 9.6 and 2.4 Hz, 1H), 7.51 (d, J = 9.2 Hz, 1H), 7.70 (s, 1H). ^{13}C NMR ($CDCl_3$) δ: 31.94, 51.38, 54.72 (2C), 55.16, 90.81, 93.49 (2C), 101.16, 112.17, 116.95, 118.45, 120.85, 125.69, 133.09, 147.38, 152.90, 160.79 (2C), 161.96. MS (ESI): $[M+1]^+$ = 371.4. Anal. calcd for $C_{20}H_{22}N_2O_5$: C, 64.85; H, 5.99; N, 7.56; found: C, 64.67; H, 5.78; N, 7.34.

*5.1.6.28. Ethyl 5-methoxy-1-methyl-3-[(3,5-dimethoxyphenyl)amino]-1H-indole-2-carboxylate (**3ab**)*. Following general procedure E, the crude residue obtained from **11g** and 3,5-dimethoxyaniline was purified by flash chromatography, using ethyl acetate:petroleum ether 2:8 (v:v) as eluent, to furnish **3ab** as a yellow solid. Yield: 45%, mp 106–107 °C. ^{1}H NMR ($CDCl_3$) δ: 1.21 (t, J = 7.2 Hz, 3H), 3.61 (s, 6H), 3.67 (s, 3H), 3.93 (s, 3H), 4.22 (q, J = 7.2 Hz, 2H), 5.89 (d, J = 2.0 Hz, 1H), 5.94 (s, 2H), 6.78 (d, J = 2.0 Hz, 1H), 7.01 (dd, J = 9.6 and 2.8 Hz, 1H), 7.51 (d, J = 9.2 Hz, 1H), 7.65 (s, 1H). ^{13}C NMR ($CDCl_3$) δ: 13.88, 31.96, 54.73 (2C), 55.18, 60.09, 90.63, 93.17 (2C), 100.86, 112.17, 116.95, 118.96, 121.28, 125.49, 132.98, 147.79, 153.06, 160.84 (2C), 161.52. MS (ESI): $[M+1]^+$ = 385.03. Anal. calcd for $C_{21}H_{24}N_2O_5$: C, 65.61; H, 6.29; N, 7.29; found: C, 65.48; H, 6.16; N, 7.09.

*5.1.6.29. n-Propyl 5-methoxy-1-methyl-3-[(3,5-dimethoxyphenyl)amino]-1H-indole-2-carboxylate (**3ac**)*. Following general procedure E, the crude residue obtained from **11i** and 3,5-dimethoxyaniline was purified by flash chromatography, using ethyl acetate:petroleum ether 2:8 (v:v) as eluent, to furnish **3ac** as a yellow solid. Yield: 42%, mp 83–85 °C. ^{1}H NMR (DMSO-d_6) δ: 0.87 (t, J = 7.2 Hz, 3H), 1.62 (m, 2H), 3.61 (s, 6H), 3.66 (s, 3H), 3.93 (s, 3H), 4.16 (q, J = 6.6 Hz, 2H), 5.89 (d, J = 1.8 Hz, 1H), 5.94 (d, J = 1.8 Hz, 2H), 6.76 (d, J = 2.2 Hz, 1H), 7.02 (d, J = 9.4 and 2.2 Hz, 1H), 7.50 (d, J = 9.4 Hz, 1H), 7.62 (s, 1H). ^{13}C NMR ($CDCl_3$) δ: 10.38, 21.36, 32.01, 54.72 (2C), 55.18, 65.67, 90.64, 93.16 (2C), 100.89, 112.19, 116.96, 118.98, 121.21, 125.48, 133.00, 147.67, 153.03, 160.82 (2C), 161.63. MS (ESI): $[M+1]^+$ = 399.3. Anal. calcd for $C_{22}H_{26}N_2O_5$: C, 66.32; H, 6.58; N, 7.03; found: C, 66.06; H, 6.36; N, 6.88.

5.2. Biological assays and computational studies

5.2.1. Cell growth conditions and antiproliferative assay

Human cervix carcinoma (HeLa), human colon carcinoma (HT29),

human breast carcinoma (MCF-7) and human promyelocytic leukemia (HL-60) cells (3–5 × 10^4 cells) and a serial (5-fold) dilution of the test compounds were added to a 96-well microtiter plate. The cells were incubated for 72 h at 37 °C in a humidified 5% CO_2 atmosphere. At the end of the incubation period, the cells were counted in a Coulter Counter (Coulter Electronics Ltd, Harpenden Herts, United Kingdom). The IC_{50} (50% inhibitory concentration) was defined as the concentration of compound that inhibited cell proliferation by 50%. The IC_{50} values represent the average (± standard deviation) of three independent experiments. Human peripheral blood mononuclear cells (PBMC) were obtained from healthy donors by centrifugation with Ficoll-Paque Plus (GE Healthcare Bio-Sciences AB, Uppsala).

5.2.2. Effects on tubulin polymerization and on colchicine binding to tubulin

Bovine brain tubulin was purified as described previously [47]. To evaluate the effect of the compounds on tubulin assembly *in vitro* [48], varying concentrations were preincubated with 10 μM tubulin in 0.8 M glutamate buffer at 30 °C and then cooled to 0 °C. After addition of GTP, the mixtures were transferred to 0 °C cuvettes in a recording spectrophotometer and warmed to 30 °C, and the assembly of tubulin was observed turbidimetrically. The IC_{50} was defined as the compound concentration that inhibited the extent of assembly by 50% after a 20 min incubation. The capacity of the test compounds to inhibit colchicine binding to tubulin was measured as described earlier [49], except that the reaction mixtures contained 0.5 μM tubulin, 5 μM [^{3}H] colchicine and 5 or 0.5 μM test compound.

5.2.3. Molecular modeling

All molecular docking studies were performed on a Viglen Genie Intel®Core™ i7-3770 vPro CPU@ 3.40 GHz × 8 running Ubuntu 14.04. Molecular Operating Environment (MOE) 2018.10 [50] and Maestro (Schrödinger Release 2017-1) [51] were used as molecular modeling software. The tubulin structures were downloaded from the PDB data bank (http://www.rcsb.org/; PDB codes 5BMV, 4O2B, 5LYJ). The proteins were preprocessed using the Schrödinger Protein Preparation Wizard by assigning bond orders, adding hydrogens and performing a restrained energy minimization of the added hydrogens using the OPLS_2005 force field. Ligand structures were built with MOE 2018.10 and then prepared using the Maestro LigPrep tool by energy minimizing the structures (OPLS_2005 force field), thereby generating possible ionization states at pH 7 ± 2 and generating tautomers and low-energy ring conformers. After isolating a tubulin dimer structure, three different 12 Å docking grids (inner-box 10 Å and outer-box 22 Å) were prepared using as centroid the co-crystallized colchicine in the 4O2B structure, the co-crystallized CA-4 in the 5LYJ protein and the βAsn249 in the 5BMV structure. Ensemble docking studies were performed using the Maestro Virtual Screening Workflow tool, setting Glide SP precision as the docking score, setting six as the number of output poses per input ligand to include in the solution and retaining all good scoring states. The output poses were saved as sdf files. The docking results were visually inspected in MOE2018.10 for their ability to bind in the active site. Superposition of the tubulin crystal structures was performed using the Alignment/Superpose tool in MOE2018.10.

5.2.4. High content imaging of cell cycle distribution

HeLa cells were seeded at 5000 cells per well in 96 well clear flat bottom tissue culture plates. After overnight incubation, the cells were treated with the test compounds at six different concentrations ranging from 6.4 × 10^{-4} to 2 μM for 24 h. Cells were then fixed with 4% PFA in PBS for 10 min, washed and the nuclei stained by adding a solution of 300 nM 4′,6-diamidino-2-phenylindole (DAPI, Molecular Probes). The plates were imaged on a CX5 High Content Screening device (ThermoFisher Scientific), using the Cell Cycle Analysis bio-application. A minimal of 500 cells was imaged for each well.

5.2.5. Apoptosis assay

HeLa cells were seeded at 1500 cells per well and PBMC at 28,000 cells per well in 384 well black-walled, clear-bottomed tissue culture plates containing the test compounds at different concentrations ranging from 6.4 × 10^{-4} to 10 μM. Both IncuCyte® Caspase 3/7 Green Reagent and IncuCyte® NucLight Rapid Red were added as recommended by the supplier, and the plates were incubated and monitored at 37 °C for 3 days in an IncuCyte® (Essen BioScience Inc., Ann Arbor, MI, USA) for real-time imaging. Images were taken every 3 h, with one field imaged per well under 10x magnification. The compounds were tested in two independent experiments, with the PBMCs originating from two different blood donors.

6. Disclaimer

This research was supported in part by the Developmental Therapeutics Program in the Division of Cancer Treatment and Diagnosis of the National Cancer Institute, which includes federal funds under Contract No. HHSN261200800001E. The content of this publication does not necessarily reflect the views or policies of the Department of Health and Human Services, nor does mention of trade names, commercial products, or organizations imply endorsement by the U.S. Government.

Declaration of Competing Interest

The authors declare that they have no known competing financial interests or personal relationships that could have appeared to influence the work reported in this paper.

Acknowledgment

We wish to thank Alberto Casolari for technical assistance. AB and SF acknowledge the support of the Life Science Research Network Wales grant no. NRNPGSep14008, an initiative funded through the Welsh Government's Sêr Cymru program. SF is supported by the Sêr Cymru program which is partially funded by the European Regional Development Fund through the Welsh Government.

References

[1] A. Muroyama, T. Lechler, Microtubule organization, dynamics and functions in differentiated cells, Development 144 (2017) 3012–3021.
[2] S. Chaaban, G.J. Brouhard, A microtubule bestiary: structural diversity in tubulin polymers, Mol. Biol. Cell 28 (2017) 2924–2931.
[3] V. Nitika, K. Kapil, Microtubule targeting agents: a benchmark in cancer therapy, Curr. Drug Ther. 8 (2014) 189–196.
[4] N.G. Vindya, N. Sharma, M. Yadav, K.R. Ethiraj, Tubulins-the target for anticancer therapy, Curr. Top. Med. Chem. 15 (2015) 73–82.
[5] I. Ojima, B. Lichtenthal, S. Lee, C. Wang, X. Wang, Taxane anticancer agents: a patent perspective, Expert Opin. Ther. Pat. 26 (2016) 1–20.
[6] Y.N. Cao, L.L. Zheng, D. Wang, X.X. Liang, F. Gao, X.L. Zhou, Recent advances in microtubule-stabilizing agents, Eur. J. Med. Chem. 143 (2018) 806–828.
[7] A.D. Tangutur, D. Kumar, K.V. Krishna, S. Kantevari, Microtubule targeting agents as cancer chemotherapeutics: an overview of molecular hybrids as stabilizing and destabilizing agents, Curr. Top. Med. Chem. 17 (2017) 2523–2537.
[8] D. Bates, A. Eastman, Microtubule destabilising agents: far more than just antimitotic anticancer drugs, Br. J. Clin. Pharmacol. 83 (2017) 255–268.
[9] C.C. Rohena, S.L. Mooberry, Recent progress with microtubule stabilizers: new compounds, binding modes and cellular activities, Nat. Prod. Rep. 31 (2014) 335–355.
[10] W. Li, H. Sun, S. Xu, Z. Zhu, J. Xu, Tubulin inhibitors targeting the colchicine binding site: a perspective of privileged structures, Future Med. Chem. 9 (2017) 1765–1794.
[11] R. Alvarez, M. Medarde, R. Pelaez, New ligands of the tubulin colchicine site based on X-ray structures, Curr. Top. Med. Chem. 14 (2014) 2231–2252.

[12] M. Dong, F. Liu, H. Zhou, S. Zhai, B. Yan, Novel natural product- and privileged scaffold-based tubulin inhibitors targeting the colchicine binding site, Molecules 21 (2016) 1375–1400.
[13] G.R. Pettit, S.B. Singh, E. Hamel, C.M. Lin, D.S. Alberts, D. Garcia-Kendall, Isolation and structure of the strong cell growth and tubulin inhibitor combretastatin A-4, Experientia 45 (1989) 209–211.
[14] G.R. Pettit, S.B. Singh, M.R. Boyd, E. Hamel, R.K. Pettit, J.M. Schmidt, F. Hogan, Antineoplastic agents 291. Isolation and synthesis of combretastatins A-4, A-5, and A-6, J. Med. Chem. 38 (1995) 1666–1672.
[15] A.T. Mc Gown, B.W. Fox, Differential cytotoxicity of combretastatins A1 and A4 in two daunorubucin-resistant P388 cell lines, Cancer Chemother. Pharmacol. 26 (1990) 79–81.
[16] E.B. Garon, J.D. Neidhart, N.Y. Gabrail, M.R. de Oliveira, J. Balkissoon, F. Kabbinavar, A randomized Phase II trial of the tumor vascular disrupting agent CA4P (fosbretabulin tromethamine) with carboplatin, paclitaxel, and bevacizumab in advanced nonsquamous non-small-cell lung cancer, Onco. Targets Ther. 9 (2016) 7275–7283.
[17] M.J. Perez-Perez, E.M. Priego, O. Bueno, M.S. Martins, M.D. Canela, S. Liekens, Blocking blood flow to solid tumors by destabilizing tubulin: an approach to targeting tumor growth, J. Med. Chem. 59 (2016) 8685–8711.
[18] E. Porcù, R. Bortolozzi, G. Basso, G. Viola, Recent advances in vascular disrupting agents in cancer therapy, Future Med. Chem. 6 (2014) 1485–1498.
[19] S.N.A. Bukhari, G.B. Kumar, H.M. Revankar, H.L. Qin, Development of combretastatins as potent tubulin polymerization inhibitors, Bioorg. Chem. 72 (2017) 130–147.
[20] P.O. Patil, A.G. Patil, R.A. Rane, P.C. Patil, P.K. Deshmukh, S.B. Bari, D.A. Patil, S.S. Naphade, Recent advancement in discovery and development of natural product combretastatin-inspired anticancer agents, Anticancer Agents Med. Chem. 15 (2015) 955–969.
[21] R. Kaur, G. Kaur, R.K. Gill, R. Soni, J. Bariwal, Recent developments in tubulin polymerization inhibitors: an overview, Eur. J. Med. Chem. 87 (2014) 89–124.
[22] Y. Shan, J. Zhang, Z. Liu, M. Wang, Y. Dong, Developments of combretastatin A-4 derivatives as anticancer agents, Curr. Med. Chem. 18 (2011) 523–538.
[23] A. Chaudari, S.N. Pandeya, P. Kumar, P.P. Sharma, S. Gupta, N. Soni, K.K. Verma, G. Bhardwaj, Combretastatin A-4 analogues as anticancer agents, Mini Rev. Med. Chem. 12 (2007) 1186–1205.
[24] I.E.L.M. Kuppens, Current status of the art of new tubulin inhibitors in the clinic, Curr. Clin. Pharmacol. 1 (2006) 47–70.
[25] R.J. van Vuuren, M.H. Visagie, A.E. Theron, A.M. Joubert, Antimitotic drugs in the treatment of cancer, Cancer Chemother. Pharmacol. 76 (2015) 1101–1112.
[26] Y.M. Liu, H.L. Chen, H.Y. Lee, J.P. Liou, Tubulin inhibitors: a patent review, Expert Opin. Ther. Pat. 24 (2014) 69–88.
[27] J.J. Field, A. Kanakkanthara, J.H. Miller, Microtubule-targeting agents are clinically successful due to both mitotic and interphase impairment of microtubule function, Bioorg. Med. Chem. 22 (2014) 5050–5059.
[28] R. Patil, S.A. Patil, K.D. Beaman, S.A. Patil, Indole molecules as inhibitors of tubulin polymerization: potential new anticancer agents, an update (2013–2015), Future Med. Chem. 8 (2016) 1291–1316.
[29] A. Brancale, R. Silvestri, Indole, a core nucleus for potent inhibitors of tubulin polymerization, Med. Res. Rev. 27 (2007) 209–238.
[30] J.-P. Liou, Y.-L. Chang, F.-M. Kuo, C.-W. Chang, H.Y. Tseng, C.-C. Wang, Y.-N. Yang, J.-Y. Chang, S.-J. Lee, H.-P. Hsieh, Concise synthesis and structure-activity relationships of combretastatin A-4 analogues, 1-aroylindoles and 3-aroylindoles, as novel classes of potent antitubulin agents, J. Med. Chem. 47 (2004) 4247–4257.
[31] J.-P. Liou, N. Mahindroo, C.-W. Chang, F.-M. Guo, S.-J. Lee, U.-K. Tan, T.-K. Yeh, C.-C. Kuo, Y.-W. Chang, P.-H. Lu, Y.-S. Tung, K.-T. Lin, J.-Y. Chang, H.-P. Hsieh, Structure-activity relationship studies of 3-aroylindoles as potent antimititotic agents, Chem. Med. Chem. 1 (2006) 1106–1118.
[32] W. Li, H. Sun, F. Xu, W. Shuai, J. Liu, S. Xu, H. Yao, C. Ma, Z. Zhu, J. Xu, Synthesis, molecular properties prediction and biological evaluation of indole-vinyl sulfone derivatives as novel tubulin polymerization inhibitors targeting the colchicine binding site, Bioorg. Chem. 85 (2019) 49–59.
[33] D.K. Sigalapalli, V. Pooladanda, P. Singh, M. Kadagathur, S.D. Guggilapu, J.L. Uppu, N.D. Tangellamudi, P.K. Gangireddy, C. Godugu, N.B. Bathinia, Discovery of certain benzyl/phenethyl thiazolidinone-indole hybrids as potential anti-proliferative agents: Synthesis, molecular modeling and tubulin polymerization inhibition study, Bioorg. Chem. 92 (2019) 103188.
[34] W. Li, W. Shuai, H. Sun, F. Xu, Y. Bi, J. Xu, C. Ma, H. Yao, Z. Zhu, S. Xu, Design, synthesis and biological evaluation of quinoline-indole derivatives as anti-tubulin agents targeting the colchicine binding site, Eur. J. Med. Chem. 163 (2019) 428–442.
[35] Giuseppe La Regina, Taradas Sarkar, Ruoli Bai, Michael C. Edler, Roberto Saletti, Antonio Coluccia, Francesco Piscitelli, Lara Minelli, Valerio Gatti, Carmela Mazzoccoli, Vanessa Palermo, Cristina Mazzoni, Claudio Falcone, Anna Ivana Scovassi, Vincenzo Giansanti, Pietro Campiglia, Amalia Porta, Bruno Maresca, Ernest Hamel, Andrea Brancale, Ettore Novellino, Romano Silvestri, New arylthioindoles and related bioisosteres at the sulfur bridging group. 4. Synthesis, tubulin polymerization, cell growth inhibition, and molecular modeling studies, J. Med. Chem. 52 (23) (2009) 7512–7527 https://pubs.acs.org/doi/10.1021/jm900016thttps://doi.org/10.1021/jm900016t.
[36] G. De Martino, G. La Regina, A. Coluccia, M.C. Edler, M.C. Barbera, A. Brancale, E. Wilcox, E. Hamel, M. Artico, R. Silvestri, Arylthioindoles, potent inhibitors of tubulin polymerization, J. Med. Chem. 47 (2004) 6120–6123.
[37] G. De Martino, M.C. Edler, G. La Regina, A. Coluccia, M.C. Barbera, D. Barrow, R.I. Nicholson, G. Chiosis, A. Brancale, E. Hamel, M. Artico, R. Silvestri, New arylthioindoles: potent inhibitors of tubulin polymerization. 2. Structure-activity relationships and molecular modeling studies, J. Med. Chem. 49 (2006) 947–954.
[38] P.C. Diao, Q. Li, M.J. Hu, Y.F. Ma, W.W. You, K.H. Hong, P.L. Zhao, Synthesis and biological evaluation of novel indole-pyrimidine hybrids bearing morpholine and thiomorpholine moieties, Eur. J. Med. Chem. 134 (2017) 110–118.
[39] P. Chen, Y.X. Zhuang, P.C. Diao, F. Yang, S.Y. Wu, L. Lu, W.W. You, P.L. Zhao, Synthesis, biological evaluation, and molecular docking investigation of 3-amidoindoles as potent tubulin polymerization inhibitors, Eur. J. Med. Chem. 162 (2019) 525–533.
[40] Schrödinger Release 2017-1: Glide, Schrödinger, LLC, New York, NY, 2017.
[41] Y. Wang, F.W. Benz, Y. Wu, Q. Wang, Y. Chen, X. Chen, H. Li, Y. Zhang, R. Zhang, J. Yang, Structural insights into the pharmacophore of vinca domain inhibitors of microtubules, Mol. Pharmacol. 89 (2016) 233–242.
[42] A.E. Prota, F. Danel, F. Bachmann, K. Bargsten, R.M. Buey, J. Pohlmann, S. Reinelt, H. Lane, M.O. Steinmetz, The novel microtubule-destabilizing drug BAL27862 binds to the colchicine site of tubulin with distinct effects on microtubule organization, J. Mol. Biol. 426 (2014) 1848–1860.
[43] R. Gaspari, A.E. Prota, K. Bargstem, A. Cavalli, M.O. Steinmetz, Structural basis of *cis*- and *trans*-combretastatin binding to tubulin, Chem. 2 (2017) 102–113.
[44] J.R. Harjani, A.X. Tang, R.S. Norton, J.B. Baell, A new methodology for the synthesis of 3-amino-1*H*-indole-2-carboxylates, Tetrahedron 70 (2014) 8047–8055.
[45] W. Youngsaye, C. Dockendorff, B. Vincent, C.L. Hartland, J.A. Bittker, S. Dandapani, M. Palmer, L. Whitesell, S. Lindquist, S.L. Schreiber, B. Munoz, Overcoming fluconazole resistance in *Candida albicans* clinical isolates with tetracyclic indoles, Bioorg. Med. Chem. Lett. 22 (2012) 3362–3365.
[46] A.S. Shestakov, K.S. Shikhaliev, O.E. Sidorenko, V.G. Kartsev, S.V. Simakov, Methyl 3-amino-1*H*-indole-2-carboxylates in the synthesis of 5*H*-pyrimido[5,4-*b*]indole derivatives, Russ. J. Org. Chem. 45 (2009) 777–782.
[47] E. Hamel, C.M. Lin, Separation of active tubulin and microtubule-associated proteins by ultracentrifugation, and isolation of a component causing the formation of microtubule bundles, Biochemistry 23 (1984) 4173–4184.
[48] E. Hamel, Evaluation of antimitotic agents by quantitative comparisons of their effects on the polymerization of purified tubulin, Cell Biochem. Biophys. 38 (2003) 1–21.
[49] P. Verdier-Pinard, J.-Y. Lai, H.-D. Yoo, J. Yu, B. Marquez, D.G. Nagle, M. Nambu, J.D. White, J.R. Falck, W.H. Gerwick, B.W. Day, E. Hamel, Structure-activity analysis of the interaction of curacin A, the potent colchicine site antimitotic agent, with tubulin and effects of analogs on the growth of MCF-7 breast cancer cells, Mol. Pharmacol. 53 (1998) 62–67.
[50] ULC, C. C. G. Molecular Operating Environment (MOE), 2018.10, 1010 Sherbooke St. West, Suite #910, Montreal, QC, Canada, H3A 2R7, 2018.
[51] Schrödinger Release 2017-1: Maestro, Schrödinger, LLC, New York, NY, 2017.